Journal of Environmental Management 165 (2016) 31–52

Contents lists available at ScienceDirect

Journal of Environmental Management

journal homepage: www.elsevier.com/locate/jenvman

Research article

# Modeling phytoplankton community in reservoirs. A comparison between taxonomic and functional groups-based models

Jimena Di Maggio [a, c], Carolina Fernández [b], Elisa R. Parodi [b, d], M.Soledad Diaz [a, c], Vanina Estrada [a, c, *]

[a] PLAPIQUI, Planta Piloto de Ingeniería Química (UNS–CONICET), Camino La Carrindanga Km 7, B8000FWB Bahía Blanca, Argentina
[b] IADO, Instituto Argentino de Oceanografía (CONICET-UNS), Camino La Carrindanga km 7, B8000FWB Bahía Blanca, Argentina
[c] Departamento de Ingeniería Química, Universidad Nacional del Sur, Alem 1253, B8000ICN Bahía Blanca, Argentina
[d] Departamento de Biología, Bioquímica y Farmacia, Universidad Nacional del Sur, San Juan 670, B8000ICN Bahía Blanca, Argentina

ARTICLE INFO

*Article history:*
Received 6 August 2014
Received in revised form
21 July 2015
Accepted 20 August 2015
Available online 23 September 2015

*Keywords:*
Phytoplankton community
Dynamic parameter estimation
Water quality mathematical model
Phytoplankton functional groups

ABSTRACT

In this paper we address the formulation of two mechanistic water quality models that differ in the way the phytoplankton community is described. We carry out parameter estimation subject to differential-algebraic constraints and validation for each model and comparison between models performance. The first approach aggregates phytoplankton species based on their phylogenetic characteristics (Taxonomic group model) and the second one, on their morpho-functional properties following Reynolds' classification (Functional group model). The latter approach takes into account tolerance and sensitivity to environmental conditions. The constrained parameter estimation problems are formulated within an equation oriented framework, with a maximum likelihood objective function. The study site is Paso de las Piedras Reservoir (Argentina), which supplies water for consumption for 450,000 population. Numerical results show that phytoplankton morpho-functional groups more closely represent each species growth requirements within the group. Each model performance is quantitatively assessed by three diagnostic measures. Parameter estimation results for seasonal dynamics of the phytoplankton community and main biogeochemical variables for a one-year time horizon are presented and compared for both models, showing the functional group model enhanced performance. Finally, we explore increasing nutrient loading scenarios and predict their effect on phytoplankton dynamics throughout a one-year time horizon.



## 1. Introduction

Ecological and environmental factors continuously interact so that the planktonic habitat never reaches the equilibrium for which only one species would be favored (Scheffer et al., 2003; Wyatt, 2013). External factors such as fluctuations in the environment, periodic forcing and spatial heterogeneity, as well as self-organizing mechanisms seem to be the cause of non-equilibrium dynamics allowing coexistence of many species (Roy and Chattopadhyay, 2007). Grime (1979) explained the co-existence of phytoplankton species through the CSR (Competitor-Stress tolerator-Ruderals) theory. This theory is based on the idea that spatial and temporal environmental heterogeneity creates a complex mosaic of microhabitats allowing a broad suite of strategies to co-exist. In aquatic ecosystems, such as lakes and reservoirs, phytoplankton communities are highly diverse and hundreds of phytoplankton species coexist. However, a usual approach in lake models is to represent phytoplankton biomass through a single variable that describes the major seasonal pattern of total phytoplankton (Hongping and Yong, 2003; Zhang et al., 2004; Ito et al., 2010; del Barrio Fernandez et al., 2012). Also, the use of taxonomic criteria to assign plankton species to a group that, in turn, is included as an output variable has been widely applied in lake modeling (e.g. Riley and Stefan, 1988; Sagehashi et al., 2000; Bowen and Hieronymus, 2003; Romero et al., 2004; Arhonditsis and Brett, 2005a; Mooij et al., 2007; Rigosi et al., 2011). Some authors model blooming species of cyanobacteria such as *Oscillatoria agardhii* (Montealegre et al., 1995), *Planktothrix rubescens* (Omlin et al., 2001a) and *Microcystis aeruginosa* (Bonnet and Poulin, 2002)

* Corresponding author. Planta Piloto de Ingeniería Química (PLAPIQUI) CC 717, Camino La Carrindanga Km 7, B8000FWB Bahía Blanca, Argentina.
*E-mail address:* vestrada@plapiqui.edu.ar (V. Estrada).

http://dx.doi.org/10.1016/j.jenvman.2015.08.027
0301-4797/

separately from the rest of the phytoplankton community. On the other hand, a few authors have proposed phytoplankton classification based on different properties (Reynolds et al., 2002; Friedrichs et al., 2007; Salmaso and Padisák, 2007; Mieleitner and Reichert, 2008; Kruk et al., 2010; Segura et al., 2013). Reynolds' approach (Reynolds et al., 2002; Padisak et al., 2009) aggregates phytoplankton species into 38 functional groups based on their morphology, survival strategies and environmental tolerance and sensitivity. This classification has been recently applied to a wide range of aquatic environments such as deep lakes (Salmaso and Padisak, 2007), temperate lakes (Huszar and Caraco, 1998), eutrophic lakes (Padisák and Reynolds, 1998; Fonseca and Bicudo, 2008) tropical coastal lagoons (Alves-de-Souza et al., 2006) and marine environments (Alves-de-Souza et al., 2008; Smayda and Reynolds, 2001, 2003). Kruk et al. (2011) studied 211 lakes worldwide ranging from subpolar to tropical regions, concluding that phytoplankton biomass can be better predicted from environmental variables using the morpho-functional classification than considering the taxonomic group classification.

In this work, we formulate two mechanistic water quality models, whose main difference is the representation of phytoplankton community. The first model aggregates phytoplankton species based on their taxonomic characteristics and the second one, on their morpho-functional properties following Reynolds' classification. We carry out parameter estimation subject to differential algebraic constraints and validation for both models, using collected data from Paso de las Piedras Reservoir (Argentina), along one year and a half. Finally, we compare both models performance and discuss the convenience of including additional complexity in phytoplankton community representation. This paper is structured as follows: Section 2 provides a brief description of the study site and sampling methods for data used in model calibration and validation; Section 3 describes both water quality models and the methodology for solving the parameter estimation problem, as well as statistical tests of model performance. Section 4 presents numerical results and discussion. Finally; Section 5 presents conclusions and future work.

## 2. Material and methods

### 2.1. Case study

Paso de las Piedras Reservoir is located in the south of Buenos Aires Province, in Argentina (38–39°S, 61–62°W) (Fig. 1). This artificial water body was built in 1978 by damming Sauce Grande River in its confluence with El Divisorio Stream, to supply drinking water to more than 450,000 inhabitants of two cities and for industrial activities at a petrochemical complex nearby. The reservoir has a surface area of 36 $km^2$, with a mean depth of 8.2 m and a retention time of 4 years. It is a non-stratified lake, mainly due to wind effects (intense and constant essentially in spring and summer), low topology of the surrounding area and the large retention time (Intartaglia and Sala, 1989). Furthermore, the reservoir is eutrophic-hypereutrophic as result of high nutrient loading from several diffuse sources (Fernandez et al., 2009). Climatic factors, as well as nutrient concentration, give rise to recurrent phytoplankton blooms during summer and early autumn (Intartaglia and Sala, 1989; Parodi et al., 2004; Fernandez et al., 2009) which cause severe problems in water supply.

### 2.2. Sampling

Sample collection was carried out between January and December 2004. Four sampling sites were considered: $S_1$ (in the water intake tower of the purifying plant), $S_3$ (next to El Divisorio Creek), $S_2$ and $S_4$ in coastal zones (Fig. 1). Samples were taken at two depths (0.5 and 10 m).

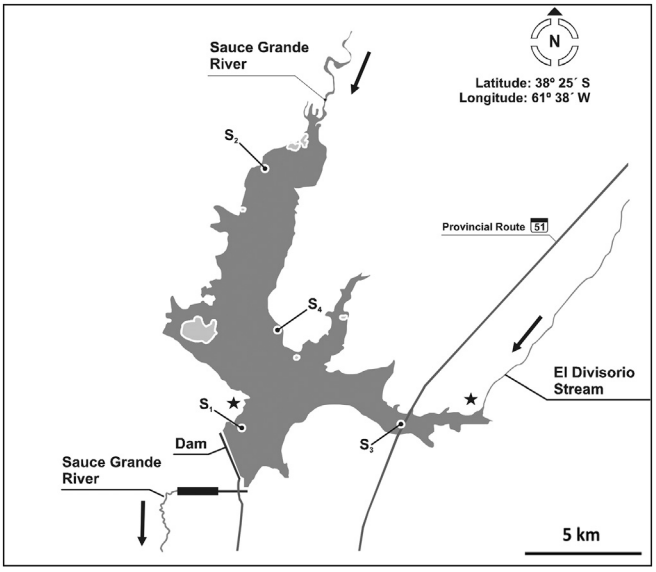


**Fig. 1.** Paso de las Piedras Reservoir. $S_1$, $S_2$, $S_3$ and $S_4$: sampling stations and (★) meteorological station.

When working with dynamic systems, it is necessary to take into account the variable with fastest time response to determine if the sampling frequency is adequate to represent the dynamics of the system (Jørgensen et al., 1981; Hangos and Cameron, 2001). Fig. 2 shows cyanobacteria dynamics as obtained with a monthly frequency (mid-month) and a twice a week frequency, respectively. As it can be seen, in winter cyanobacteria concentration variability is low, so the sampling frequency can be lower, while during the warm periods it can be underestimated. Based on these considerations, biological variables, temperature and dissolved oxygen were sampled twice a week; while nutrients were sampled once a week. Samples for qualitative analysis were taken with a 30-μm-mesh plankton net and a van Dorn bottle. Some samples were not fixed, while others were fixed immediately with 4% formaldehyde. Samples for quantitative analyses were collected with a van Dorn bottle and fixed immediately with Lugol's solution.

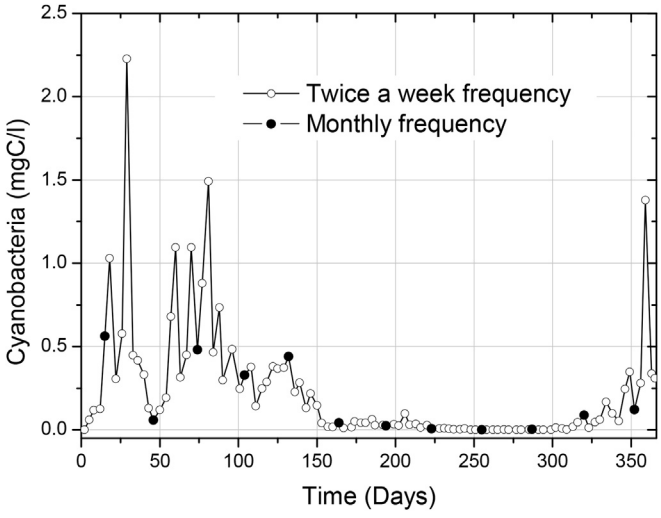


**Fig. 2.** Cyanobacteria biomass concentration vs. time for two sampling frequencies.

For qualitative analysis, samples were observed under an optical microscope Nikon Eclipse 80i with a digital DXM1200F camera. Phytoplankton was identified using Komárek & Anagnostidis keys (1989,1999, 2005), Komárek and Fott (1983), Hindák (1988, 1990), and Krammer and Lange-Bertalot (1986, 1988,1991a, b). The Utermöhl method (1958) was used to quantify phytoplankton under an inverted microscope (Wild) with a magnification of x400. Sedimentation time was more than 12 h. The number of settling units counted in each individual sample varied according to the species accumulation curve; the same chamber volume (10 ml) was used throughout the study and at least 40 fields were counted for each chamber (Rott, 1981). The cells were discriminated to the species level, wherever possible. Cell counts were converted to biovolume according to their size and geometric form (Hillebrand et al., 1999; Sun and Liu, 2003). We calculated each species biovolume, by measuring the dimension of 30 cells of each species and calculating its mean value. Furthermore, as ecological models require the formulation of mass balances, phytoplankton biomass is represented in these models by its carbon content. For this reason, carbon content of phytoplankton cells was calculated based on biovolume, following Smayda (1978):

$$log_{10}C = 0.758(log_{10}V) - 0.422 \text{ for diatoms} \quad (1)$$

$$log_{10}C = 0.866(log_{10}V) - 0.460 \text{ for other } taxa \quad (2)$$

where $V$ is the cell volume in $\mu m^3$ and $C$ is the carbon concentration in pg/cell.

Water samples for nutrient analysis were collected with a van Dorn bottle at the same sites and depth as for phytoplankton; they were stored in darkness at 4 °C and processed within 24–48 h. Nitrate ($NO_3^-$), nitrite ($NO_2^-$), ammonium ($NH_4^+$), total phosphorus (TP), soluble reactive phosphorus (SRP) and silica were analyzed in the Water Authority Laboratory (ADA), Buenos Aires, following the methods described by the American Public Health Association (1992). Furthermore, *in situ* measurements of selected chemical and physical characteristics were conducted, including electrical conductivity, temperature and pH using a Horiba U-10 multisensor. Two meteorological stations located next to the reservoir area, provided data of air temperature, wind speed and direction and precipitations (Fig. 1). The Laboratory of Hydraulic at Universidad Nacional del Sur and the Water Authority (ADA) provided these data, along with data on reservoir water volume and level, and tributary flows and nutrient concentrations.

## 3. Mathematical model

### 3.1. Water quality model

We propose mechanistic water quality models describing the main biogeochemical processes within a water body. The models include mass balances for phytoplankton, $NO_3^-$, $NH_4^+$, SRP, OP and ON, DO and BOD, resulting in a complex system of partial differential-algebraic equations (PDAE) that takes into account temporal and spatial concentrations variation.

An important assumption is the consideration of averaged horizontal concentrations. Thus, the differences in spatial concentrations are only along the vertical coordinate (Fig. 3). This approach has been adopted in many mechanistic water quality models (Omlin et al., 2001a, b; Zhang et al., 2004; Arhonditsis et al., 2006). The small differences in data collected during bloom periods between sampling stations (8, 9 and 12% average differences in nitrate, phosphate and total phytoplankton concentrations, respectively) justify this assumption (Estrada et al., 2009a).

To transform the PDAE system into a set of ordinary differential-algebraic equations (DAE), the water column is spatially discretized into two horizontal layers (upper and lower). A bi-layer description is appropriate for water bodies that have thermocline, particularly during the spring phytoplankton bloom and the subsequent stratification period in summer (Arhonditsis and Brett, 2005a; Zhang et al., 2004). Two layers discretization has been adopted in several ecological models, mainly in order to represent differences between the epilimnion and hypolimnion in stratified lakes during summer and winter periods (Rajar and Cetina, 1997; Zhang et al., 2004; Osidele and Beck, 2004; Arhonditsis and Brett, 2005a). Even though in our case study there is no thermocline that prevents mixing along the water column, light intensity decreases with depth, creating differences in the primary productivity between layers, thus justifying the vertical spatial discretization. The annual mean compensation point in Paso de las Piedras Reservoir (calculated as 2 x Secchi depth) is 3.12 m while the mean depth of the lake is 8.2 m indicating that the lower layer has a light intensity lower than the required for phytoplankton growth and respiration becomes the prevalent metabolic process.

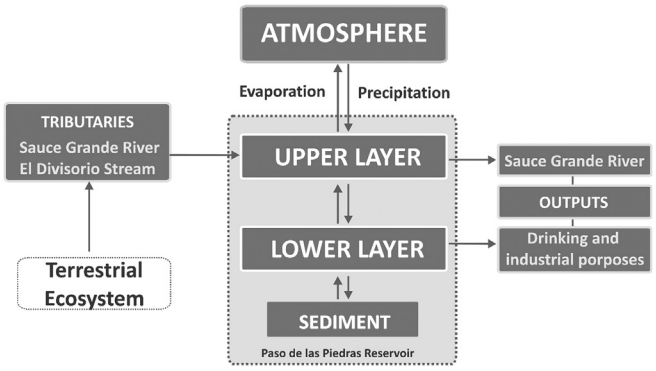


**Fig. 3.** Simplified diagram of the Paso de las Piedras Reservoir water quality model.

Table 1 shows component mass balances formulated for Paso de las Piedras Reservoir water quality model (Eqs. (1) and (2)) and a water mass balance that takes into account tributaries and precipitation water inputs, evaporation and outputs for drinking water and industrial proposes (Eq. (3)). Dynamic mass balances in each spatial layer include component inputs from tributaries (Term 1 in Eq. (1)), outputs for both potabilization and industrial purposes and the river itself (Term 1 in Eq. (2) and term 2 in Eq. (1), respectively), generation and consumption (Term 3 in Eq. (1) and term 2 in Eq. (2)), and transference between layers (Term 4 in Eq. (1) and term 3 in Eq. (2)), also accounting for lake volume variability (through upper layer height variability, term 5 in Eq. (1)). Algebraic equations represent the generation/consumption terms and the forcing functions. These ones are approximated with sinusoidal functions and correspond to temperature, solar radiation, precipitations, evaporation, tributaries inflows, phosphorus and nitrogen concentration in tributaries, and silica concentration profiles. The corresponding nomenclature is shown in Table 2. Appendix A shows the equations that describe phytoplankton, nutrients and dissolved oxygen dynamics. A more detailed explanation of these rate equations can be found in Estrada et al. (2009a, b).

### 3.2. Phytoplankton succession modeling

In this section we briefly describe the alternative approaches to model phytoplankton community, either based on taxonomic or functional groups. In both cases, the different groups differ in their competition strategies related to available resources and their metabolic rates, which include the following parameters:

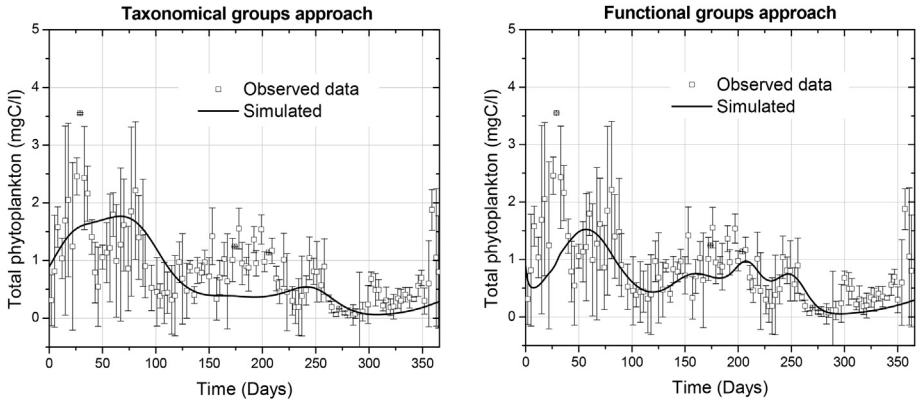


**Fig. 4.** Calibration. Observed data (mean and standard deviation) for the four sampling stations and simulation time series for total phytoplankton biomass for taxonomic and functional group approaches.

**Table 1**
Mass balance equations for water quality model of Paso de las Piedras Reservoir. For taxonomic approach $j = Cy$, *Chl* and *Diat* and for functional group approach $j = C, D, F, H1, J, M$ and $P$.

Upper layer ($U$)

$$\frac{dC_{Uj}}{dt} = \sum_k \underbrace{\frac{Q_{IN,Uk}}{V_U} C_{IN,Ujk}}_{1} - \underbrace{\frac{Q_{OUT,U}}{V_U} C_{Uj}}_{2} + \underbrace{r_{Uj}}_{3} - \underbrace{\frac{k_d A}{\Delta h V_U}(C_{Uj} - C_{Lj})}_{4} - \underbrace{\frac{C_{Uj}}{h_U}\frac{dh}{dt}}_{5} \quad (1)$$

1 Tributaries inputs (Sauce Grande River and El Divisorio Stream)
2 Sauce Grande River output
3 Generation/consumption term
4 Exchange between layers (Fick law)
5 Upper layer volume variation

Lower layer ($L$)

$$\frac{dC_{Lj}}{dt} = \underbrace{-\frac{Q_{OUT,L}}{V_L} C_{Lj}}_{1} + \underbrace{r_{Lj}}_{2} + \underbrace{\frac{k_d A}{\Delta h V_L}(C_{Uj} - C_{Lj})}_{3} \quad (2)$$

1 Outputs for drinking water and industrial proposes
2 Generation/consumption term
3 Exchange between layers (Fick law)

Total water balance

$$\frac{dh}{dt} = \frac{1}{A}\left[Q_{rain} - Q_{evap} + \sum_k Q_{IN,k} - \sum_m Q_{OUT,m}\right] \quad (3)$$

$j$ refers to each phytoplankton group, i.e.: cyanobacteria, chlorophyta and diatoms for the taxonomical group approach and group F, J, H1, P, D, M and C for the functional group approach
$k$ refers to tributaries
$m$ refers to each output of the reservoir

maximum growth rate ($k_{j,growth}$), respiration rate ($k_{j,resp}$), mortality rate ($k_{j,death}$), settling velocity ($k_{j,settling}$), optimal temperature ($T_{opt,j}$) and light intensity for growth ($I_{opt,j}$).

Based on relative abundance of phytoplankton biomass in our case study, three *taxa* are considered in the taxonomic group-based model: cyanobacteria (Cy), chlorophytes (Chl) and diatoms (Diat) (in Table 1, $j =$ *Cy*, *Chl*, *Diat*). Cyanobacteria are modeled as *K*-selected organisms (Reynolds, 2006). These organisms are characterized by low metabolic rates and growth, high optimal growth temperatures and irradiances, low sedimentation rates and low vulnerability to grazing by herbivorous zooplankton. On the other hand, diatoms are parameterized as *R*-selected organisms which tend to have high metabolic, growth and sedimentation rates, low optimal temperature and irradiance requirements. Chlorophytes are intermediate between cyanobacteria and diatoms in terms of their competitive strategies against available resources (Zhao et al., 2008b).

In the functional group-based approach, we combine the species contributing with more than 5% to the total biomass into functional groups, using Reynolds' criteria, following Padisák et al. (2009), Reynolds (2006) and Reynolds et al. (2002). Such functional groups form clusters of species with more or less precisely defined demands for different combinations of physicochemical and biological properties (depth of mixing layer, light, temperature, P, N, Si, $CO_2$ and grazing pressure) of the lake environment. Once the species of the phytoplankton community of Paso de las Piedras Reservoir are classified based on Reynolds' groups (Table 3), the most representative groups throughout the year are selected according to their relative biomass contribution to total phytoplankton biomass. The main functional groups included in the water quality are referred to as C, D, F, H1, J, M and P. Functional groups C and D are represented by *Cyclotella meneghiniana* and

**Table 2**
Model variables nomenclature.

| Symbol | Description | Unit |
|---|---|---|
| $C_j$ | Concentration of the component $j$ | mg/L |
| $U$ | Upper layer | |
| $L$ | Lower layer | |
| $Q_{IN,k}$ | Tributaries inputs | L/d |
| $Q_{OUT,U}$ | Sauce Grande River output | L/d |
| $Q_{OUT,L}$ | Drinking water and industrial proposes outputs | L/d |
| $Q_{OUT,m}$ | Tributaries outputs | L/d |
| $Q_{rain}$ | Precipitation inputs | L/d |
| $Q_{evap}$ | Evaporation outputs | L/d |
| $V_U$ | Upper layer volume | L |
| $V_L$ | Lower layer volume | L |
| $h_U$ | Upper layer depth | m |
| $h_L$ | Lower layer depth | m (Fixed at 3.5) |
| $h_T$ | Total depth | m |
| $\Delta_h$ | Depth between the middle of the upper layer and the middle of the lower layer | m |
| $r_{Uj}$ | Generation/consumption term for $j$ in the upper layer | mg/L/d |
| $r_{Lj}$ | Generation/consumption term for $j$ in the lower layer | mg/L/d |
| $A$ | Lake area | $m^2$ |
| $k_d$ | Eddy diffusion rate | $m^2/d$ |
| $Z_{max}$ | Maximum depth of the reservoir | m |

**Table 3**
Main phytoplankton species of Paso de las Piedras Reservoir included in each functional group.

| FG | Specie | Taxonomic group |
|---|---|---|
| C | *Cyclotella meneghiniana* | Bacillariophyceae |
| D | *Stephanodiscus* sp. | Bacillariophyceae |
| P | *Closterium aciculare* | Zygnemaphyceae |
| | *Closterium moniliferum* | Zygnemaphyceae |
| | *Staurastrum chaetoceras* | Zygnemaphyceae |
| | *Staurastrum gracile* | Zygnemaphyceae |
| | *Aulacoseira granulata* | Bacillariophyceae |
| | *Aulacoseira granulata* var. *angustissima* | Bacillariophyceae |
| | *Navicula peregrina* | Bacillariophyceae |
| F | *Sphaerocystis schroeteri* | Chlorophyceae |
| | *Planktosphaeria gelatinosa* | Chlorophyceae |
| | *Dictyosphaerium ehrenbergianum* | Chlorophyceae |
| | *Dictyosphaerium pulchellum* | Chlorophyceae |
| | *Lagerheimia citriformis* | Chlorophyceae |
| | *Oocystella borgei* | Chlorophyceae |
| | *Oocystella lacustris* | Chlorophyceae |
| | *Oocystella marssonii* | Chlorophyceae |
| | *Oocystella parva* | Chlorophyceae |
| | *Oocystella solitaria* | Chlorophyceae |
| J | *Pediastrum duplex* var. *duplex* | Chlorophyceae |
| | *Coelastrum microporum* | Chlorophyceae |
| | *Coelastrum astroideum* | Chlorophyceae |
| | *Coelastrum indicum* | Chlorophyceae |
| H1 | *Anabaena circinalis* | Cyanobacteria |
| M | *Microcystis aeruginosa* | Cyanobacteria |
| | *Microcystis flos-aquae* | Cyanobacteria |
| | *Microcystis natans* | Cyanobacteria |
| | *Microcystis protocystis* | Cyanobacteria |

*Stephanodiscus* sp. respectively, the most abundant diatoms in the reservoir. They are typical of eutrophic and mixed waters since they are negatively affected by the onset of stratification. The F group includes non-motile but near-neutrally-buoyant colonial green algae typical of clear, deeply mixed meso-eutrophic lakes. It comprises the species: *Sphaerocystis schroeteri, Planktosphaeria gelatinosa, Dictyosphaerium ehrenbergianum, Dictyosphaerium pulchellum, Lagerheimia citriformis, Oocystella borgei, Oocystella lacustris, Oocystella marssonii, Oocystella parva, Oocystella solitaria.* H1 is the classical eutrophic, low nitrogen group, it includes nitrogen-fixing species *Dolichospermum circinalis.* Group J includes mainly non-gelatinous, non-motile Chlorococcales prominent in shallow, highly enriched systems. In Paso de las Piedras Reservoir it includes: *Pediastrum duplex* var. *dúplex, Coelastrum microporum, Coelastrum astroideum* and *Coelastrum indicum.* Group M is typical of eutrophic to hypertrophic, small-to medium-sized water bodies. It includes almost monocultures of large colonies of species such as *Microcystis aeruginosa, Microcystis flos-aquae, Microcystis natans and Microcystis protocystis.* Group P includes *R*-strategist organisms (ruderals) that tolerate light and carbon. They require a continuous or semi-continuous mixed layer of 2–3 m thickness. In Paso de las Piedras Reservoir it includes: *Closterium aciculare, Closterium moniliferum, Staurastrum chaetoceras, Staurastrum gracile, Aulacoseira granulata, A. granulata* var. *angustissima, Navicula peregrina.*

### 3.3. Parameter estimation

Complex deterministic models for aquatic ecosystems typically have a large number of parameters that are site-specific and unknown. These parameters must be tuned based on observed data of the system under study. The water quality model of Paso de las Piedras Reservoir described in Section 3 comprises a set of nonlinear differential algebraic equations (DAE) that can be represented by the following general equation:

$$f(x(t),\ \dot{x}(t), y(t), \theta\ ) = 0 \tag{3}$$

where $x(t)$ are differential state variables (Table 1), $\dot{x}(t)$ are the time derivatives, $y(t)$ are algebraic variables through which we describe the input data (temperature, solar radiation, precipitation, evaporation, tributaries inflows and the external nutrient loading), and generation/consumption terms $r_{Uj}$ and $r_{Lj}$) and $\theta$ is the set of parameters to be estimated. A set of initial conditions was defined for the differential variables with the experimental concentrations of the first sample data.

We carried out an exhaustive search on the range of the parameter values in the literature. These values are based on field studies, laboratory and modeling See Table 8).

In previous work, we performed a global sensitivity analysis on the ecological model of Paso de las Piedras Reservoir (Estrada and Diaz, 2010) to identify main parameters to which model outputs are more sensitive. Based on this study, we selected the model parameters that will be estimated (vector $\theta$). As Bennett et al. (2013) mention, sensitivity analysis is an important and useful tool on model development. We formulated the parameter estimation problem as a constrained dynamic optimization problem within an

equation oriented environment in gPROMS. The gEST tool in gPROMS (PSEnterprise, 2014) solves dynamic parameter estimation problems with two alternative performance criteria, least squares or maximum likelihood. The idea behind the maximum likelihood estimation is to determine the values of control parameters that maximize the probability of best fitting the sample data. Because the measurement errors are important in the process being observed, the maximum likelihood estimation needs not only the water quality mathematical model but also a model for measurement errors (Seinfeld and Lapidus, 1974). Assuming that these errors are independent and normally distributed, the objective function considered in this method is:

$$\varphi = \frac{M}{2} ln(2\pi) + \frac{1}{2} \min_{\theta} \left\{ \sum_{i=1}^{NE} \sum_{j=1}^{NV_i} \sum_{k=1}^{NM_{ij}} \left[ ln\left(\sigma_{ijk}^2\right) + \frac{\left(x_{ijk}^* - x_{ijk}\right)^2}{\sigma_{ijk}^2} \right] \right\} \tag{4}$$

where $M$ is the total number of measurements, $NE$ is the number of experiments, $NV_i$ is the number of measured variables in the $i$th sampling site, $NM_{ij}$ is the number of measurement of the $j$th variable in the $i$th sampling site, $\sigma_{ijk}^2$ is the variance of the $k$th measurement of variable $j$ in sampling site $i$. The optimization algorithm determines both the values of the lake model parameters and the variance model parameters ($\sigma$). If the structure of the data is known, gEST provides two alternative models for the measurement error variance: homoscedastic and heteroscedastic.

In order to specify the model variance of the measurement error, we applied Levene's test to the observed data for the four sampling stations from Paso de las Piedras Reservoir. The groups in the statistical test are cyanobacteria, chlorophytes, diatoms and inorganic nutrients concentrations and subgroups correspond to these concentrations grouped in different months.

The parameter estimation problem is formulated as:

$$\begin{aligned} &\min_{\theta} \varphi \\ &\text{subject to} \\ &\text{DAE lake model} \\ &x_i(0) = x_i^0 \\ &p^L \le p \le p^U \end{aligned} \tag{5}$$

In Eq. (5) selected parameters to be estimated ($\theta$) are the optimization variables (time independent degrees of freedom). In this approach a Nonlinear Programming problem (NLP) is formulated at the outer level, with these parameters as optimization variables. Given estimated values for these parameters, there are no degrees of freedom in the inner level, and the differential algebraic equations (DAE) system can be solved with a DAE solver; in our case, DASOLV routine (Petzold, 1982), within gPROMS (PSEnterprise, 2014). If the optimum value of the optimization problem is not found, information on objective function, constraints and their gradients is transferred to the external NLP problem, in which variables $\theta$ are updated by solving the NLP and transferred to proceed with the next inner DAE system solution. The NLP in the outer level is solved with an SQP (Successive Quadratic Programming) algorithm.

Data for calibration purposes were collected throughout an entire year (2004) twice a week for phytoplankton and physicochemical variables, and weekly for nutrients determinations. Model validation is carried out against an independent data set of Paso de las Piedras for the period between January and June of 2005 in which samples were collected fortnightly.

#### 3.3.1. Statistical evaluation of model performance

The model performance for calibration purposes has been assessed quantitatively by three diagnostic measures calculated, based on monthly average values of the main state variables (phytoplankton groups for both approaches, SRP, $NO_3^-$ and DO). Additionally, residual plots have been made.

The mean error ($ME$) (Eq. (6)) is a measure of model bias giving information on overestimation or underestimation of a variable and should be close to zero (Power, 1993). The relative error ($RE$) (Eq. (7)) characterizes the model accuracy. The index of agreement ($d$) (Eq. (8)), proposed by Willmott (1981), is a standardized measure of the degree of model prediction error and varies between 0 and 1 (Moriasi et al., 2007; Rode et al., 2007), with higher values indicating better agreement between data and model simulations.

$$ME = \frac{\sum_{i=1}^{n} \left(y_i - \widehat{y}_i\right)}{n} \tag{6}$$

$$RE = \frac{\sum_{i=1}^{n} \left|y_i - \widehat{y}_i\right|}{\sum_{i=1}^{n} y_i} \tag{7}$$

$$d = 1 - \frac{\sum_{i=1}^{n} \left(y_i - \widehat{y}_i\right)^2}{\sum_{i=1}^{n} \left(|\widehat{y}_i - \overline{y}| + |y_i - \overline{y}|\right)^2} \tag{8}$$

where $\overline{y}$ is the mean of the observed values, $y_i$ and $\widehat{y}_i$ the observed and simulated values, respectively, and $n$ the number of observations.

Residual plots show temporal distribution of residuals for state variables and give information about the unpredicted system behavior (Hangos and Cameron, 2001; Bennett et al., 2013).

## 4. Results and discussion

### 4.1. Analysis of phytoplankton biomass data

We carry out a detailed analysis of collected data from Paso de las Piedras Reservoir to define the state variables that represent phytoplankton community in the taxonomic and functional group-based models, respectively. In the first case, phytoplankton is classified into three taxonomic groups (cyanobacteria, diatoms and chlorophytes), whose observed data are shown in Fig. 5 for the sampling period (2004). These groups comprise over 90% of total phytoplankton biomass (Table 4).

In the second case, phytoplankton species are classified into 18 functional groups based on Reynolds et al. (2002). Seven of these functional groups (in Table 1, $j = F, J, H1, P, D, M, C$) are selected as state variables for the functional group model based on the criteria that their mean annual biomass exceeds 5% of the mean annual total biomass (Table 5). As in the case of the taxonomic approach, the mean monthly biomass of the selected functional groups most of the time explains up to 90% of total biomass (Table 6).

Tables 3 and 7 show the phytoplankton species included in the functional groups in the model and their main characteristics, respectively. We include the most common problem-causing algae related with drinking water supply within the selected functional groups. A survey conducted by AWWA Research Foundation (Defler and Belk, 2004) to collect information about the existing algae problems at U.S. water treatment plants (WTPs) revealed that 73% experienced algae-related problems and 90% of 126 WTPs reported taste and odor problems. Drinking water supply from Paso de las Piedras Reservoir is affected during summer and early autumn months by the appearance of unpleasant odor and flavor. The

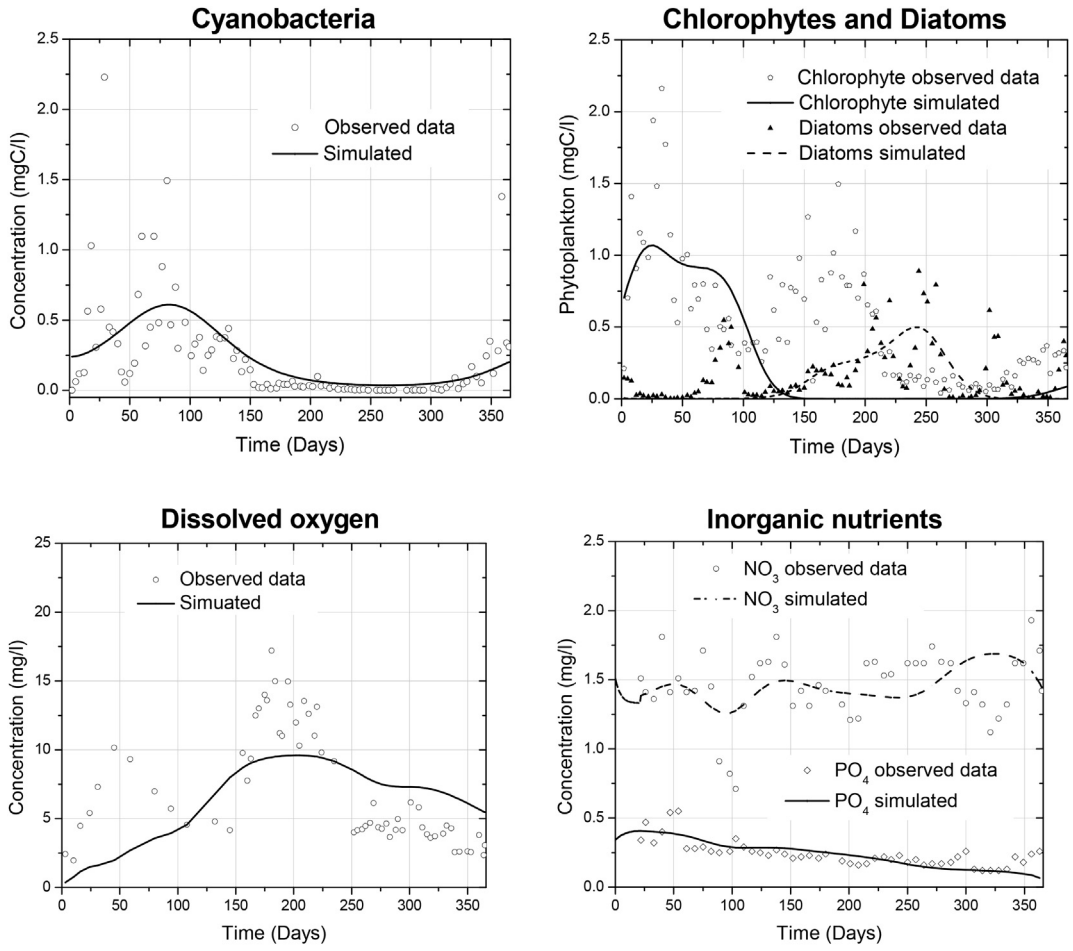


**Fig. 5.** Calibration. Observed data and simulation time series for main state variables using the taxonomic group approach model of Paso de las Piedras Reservoir.

**Table 4**
Percentage of biomass of the taxonomic groups included in the model in relation to total phytoplankton biomass in mgC/L of Paso de las Piedras Reservoir.

| TG | Jan. | Feb. | Mar. | Apr. | May | Jun. | Jul. | Aug. | Sep. | Oct. | Nov. | Dec. |
|---|---|---|---|---|---|---|---|---|---|---|---|---|
| Cyanobacteria | 32.4 | 20.8 | 48.1 | 40.0 | 26.6 | 2.8 | 3.6 | 5.8 | 0.2 | 1.2 | 13.5 | 19.4 |
| Chlorophyta | 63.4 | 77.9 | 37.4 | 44.3 | 64.7 | 77.8 | 66.1 | 82.5 | 21.7 | 33.2 | 44.5 | 57.5 |
| Diatoms | 3.5 | 0.8 | 13.7 | 15.1 | 6.2 | 17.4 | 28.0 | 5.8 | 77.2 | 48.8 | 37.7 | 19.4 |
| $\sum_{i=1}^{3}$TG | 99.2 | 99.6 | 99.2 | 99.3 | 97.6 | 97.9 | 97.7 | 94.2 | 99.1 | 83.2 | 95.7 | 96.3 |

strong odor is due to the presence of geosmin, released by *Dolichospermum circinalis* (group H1) (Dzialowski et al., 2009; Parinet et al., 2010; Ho et al., 2012). *Microcystis* (group M), other important genera of cyanobacteria in Paso de las Piedras Reservoir, is not commonly involved in taste and odor problems but it is, as in the case of *D. circinalis*, associated with the production of toxins (Defler and Belk, 2004). Certain diatoms, desmids, and dinoflagellates are able to clog the filters at WTPs because of their cell walls which persist even when the cell is dead. AWWA reported that in the 48% of the WTPs with algae-related problems, filter clogging by algae took place. *Dolichospermum* (group H1) and *Microcystis* (group M) also appear as filter clogging algae (APHA, AWWA and WPCF, 1989), but diatoms are the main algae class associated to this problem. There are two main functional groups of diatoms listed as filter-clogging algae (Palmer, 1980; Joh et al., 2011) in Paso de las Piedras Reservoir, group C, mainly represented by *Cyclotella meneghiniana,* and group D, represented by *Stephanodiscus* sp. Both of them are central diatoms with different growth requirements (silica, temperature, light, etc.), tolerances and sensitivities (Table 3). The most relevant genera included in group P (Table 7) are the filamentous diatom *Aulacoseira* and desmids *Closterium* and *Staurastrum,* all of them filter-clogging algae (Palmer, 1980; APHA, AWWA and WPCF, 1989). Even though the taxonomic approach takes into account main algae groups, it is important to note that the model based on functional groups describes with more detail the main species of phytoplankton community related to problems in drinking water supply. For example, although *Dolichospermum* and *Microcystis* (modeled as cyanobacteria in the taxonomic approach) can produce toxins, the nature and effects of these toxins are different (Carmichael, 1992, 1997), whereby it is important to model them as separated state variables.

Regarding phytoplankton succession in Paso de las Piedras Reservoir, the dominant phytoplankton species in January 2004 belong to groups P and J, with more than 80% of total biomass. Groups P and J also dominated in February 2004 accompanied by groups F and M. During mid-February and March 2004, dominated

**Table 5**
Annual mean biomass and percentage relative abundance (RA%) for functional groups (FG) based on Reynolds classification for phytoplankton species of Paso de las Piedras Reservoir.

| FG | Biomass (mgC/L) | RA% |
|---|---|---|
| F | 0.2367 | 25.07 |
| J | 0.2068 | 21.91 |
| H1 | 0.1240 | 13.14 |
| P | 0.0982 | 10.40 |
| D | 0.0707 | 7.49 |
| M | 0.0520 | 5.51 |
| C | 0.0509 | 5.39 |
| LO | 0.0461 | 4.88 |
| X1 | 0.0136 | 1.44 |
| X2 | 0.0112 | 1.18 |
| T | 0.0106 | 1.12 |
| K | 0.0065 | 0.69 |
| Y | 0.0061 | 0.65 |
| X3 | 0.0046 | 0.48 |
| XPH | 0.0033 | 0.35 |
| W2 | 0.0018 | 0.19 |
| MP | 0.0006 | 0.07 |
| N | 0.0006 | 0.06 |

Table C1 from Appendix C, determine homoscedasticity and this information is included within the parameter estimation problem (constant variance model in gPROMS).

The parameter estimation problem constrained with the water quality model (Eq. (5)) based on taxonomic groups for phytoplankton has 21 differential, 60 algebraic equations and 17 parameters to be estimated, which are shown in Table 8. The model based on functional groups has 29 differential, 108 algebraic equations and 35 parameters as degrees of freedom for the parameter estimation problem, which are also shown in Table 8. In both cases, there is an additional differential equation corresponding to the integral objective function (Eq. (4)). As compared to the model based on taxonomic groups, the second parameter estimation problem (functional group approach) has 8 differential and 48 algebraic additional equations, which are described in Table C2, from Appendix C. The increase in model size and complexity is mainly reflected in CPU time required for solution (Table C2, Appendix C).

Table 8 shows the optimal values of the 17 and 35 estimated parameters for taxonomic and functional group models, respectively. Parameter values not involved in the calibration task are listed in Appendices A and B.

**Table 6**
Percentage of biomass of the functional groups included in the model in relation to total phytoplankton biomass in mgC/L of Paso de las Piedras Reservoir.

| FG | Jan. | Feb. | Mar. | Apr. | May | Jun. | Jul. | Aug. | Sep. | Oct. | Nov. | Dec. |
|---|---|---|---|---|---|---|---|---|---|---|---|---|
| C | 0.2 | 0.5 | 0.7 | 0.4 | 0.9 | 1.2 | 24.7 | 38.6 | 2.3 | 1.7 | 8.7 | 1.6 |
| D | 3.0 | 0.0 | 0.0 | 0.0 | 0.2 | 0.0 | 1.4 | 18.6 | 74.8 | 46.5 | 28.8 | 3.7 |
| F | 18.1 | 19.2 | 9.4 | 18.4 | 35.1 | 61.9 | 52.4 | 18.9 | 10.9 | 7.6 | 13.2 | 13.7 |
| H1 | 21.3 | 7.3 | 34.6 | 0.7 | 0.5 | 0.7 | 1.9 | 1.0 | 0.2 | 0.3 | 13.4 | 40.1 |
| J | 34.2 | 54.1 | 20.6 | 17.4 | 21.7 | 9.7 | 9.3 | 14.6 | 7.6 | 12.6 | 5.5 | 8.6 |
| M | 8.6 | 10.7 | 10.7 | 7.4 | 4.6 | 0.6 | 0.1 | 0.1 | 0.0 | 0.00 | 0.1 | 4.5 |
| P | 9.1 | 2.0 | 16.2 | 18.1 | 8.2 | 18.7 | 3.2 | 2.1 | 1.4 | 5.3 | 18.4 | 21.0 |
| $\sum_{i=1}^{7} FG$ | 94.5 | 93.9 | 92.2 | 62.4 | 71.2 | 92.9 | 92.9 | 93.7 | 97.2 | 74.1 | 88.1 | 93.1 |

**Table 7**
Main characteristics of phytoplankton functional groups considered in this study (quoted from Reynolds et al., 2002; Reynolds, 2006 and Padisák et al., 2009).

| FG | Habitat template | Tolerance | Sensitivity |
|---|---|---|---|
| C | Eutrophic small- and medium-sized lakes with species sensitive to the onset of stratification | Light and C deficiencies | Si exhaustion, stratification |
| D | Shallow and enriched turbid waters, including rivers | Flushing | Nutrient depletion |
| F | Continuous or semi-continuous mixed layer of 2–3 m in thickness. Eutrophic epilimnia | Mild light and C deficiency | Stratification and silica depletion |
| H1 | Clear, deeply mixed meso-eutrophic lakes | Low nutrients | $CO_2$ deficiency and high turbidity |
| J | Shallow, mixed, highly systems (including many low-gradient rivers) | | Settling into low light |
| M | Eutrophic, both stratified and shallow lakes with low nitrogen content. | Low nitrogen, low carbon | Mixing, poor light, low phosphorus |
| P | Eutrophic to hypertrophic, small to medium-sized water bodies | High insolation | Flushing, low total light |

groups H1 and P. April was dominated by group P with a smaller contribution of groups F, J, $L_O$ and M. During May and June 2004 group P still dominated, together with group F. July and October were dominated by diatoms from groups C and D. The latter dominated until mid-November. In December, as the water temperature increased, the relative biomass of the diatom groups decreased and group P became dominant again. Collected data of the phytoplankton biomass classified by functional groups is shown in Fig. 6. As compared to the taxonomic group classification, it can be seen that phytoplankton patterns for the functional group approach are simpler and with lower data dispersion. More details on phytoplankton succession patterns and dominance of phytoplankton groups are provided in Fernandez et al. (2014).

### 4.2. Calibration, validation and ecological performance

As a first step, we have carried out Levene's test on variances of measurement errors. Numerical results, which are shown in

Table 9 presents the goodness-of-fit statistics for the calibration of taxonomic and functional group models, based on monthly averages values through the evaluation of the medium error (*ME*), the relative error (*RE*) and the index of agreement (*d*).

Fig. 4 shows total phytoplankton profiles along the time horizon considered in the calibration period for both approaches including mean and standard deviation for the data of the four sampling stations. Figures 5 to 7 show the observed data and simulated time series after parameter estimation, for the main water quality variables of both models. These figures show experimental data for the sampling station next to the intake tower ($S_1$in Fig. 1) which is considered more important in terms of water quality concerns.

The taxonomic group model provides acceptable agreement with experimental data, with cyanobacteria dynamics achieving the most satisfactory fit ($ME = -0.045$, *RE***Error! Reference source not found.** = 39.5%, *d***Error! Reference source not found.** = 0.91),

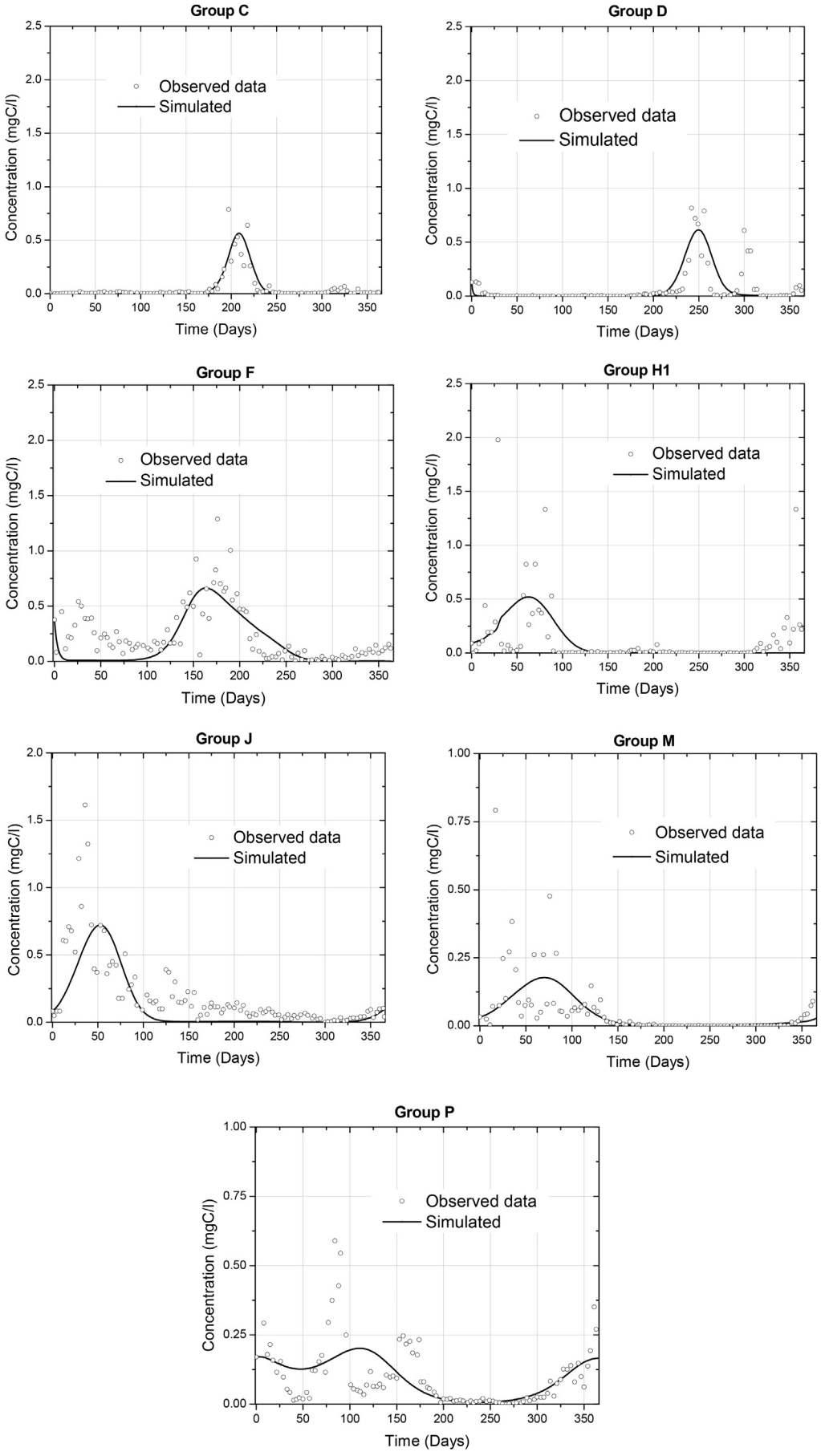


**Fig. 6.** Calibration. Observed data and simulation time series for the state variables that represent phytoplankton of Paso de las Piedras Reservoir in the functional group approach model.

**Table 8**
Optimal parameter set for taxonomic and functional group models. $k_{j,growth}$: maximum growth rate ($day^{-1}$), $k_{j,death}$: mortality rate ($day^{-1}$), $I_{optj}$: optimal light intensity for growth ($Wm^{-2}$), $K_{Pj}$: half-saturation constant for phosphorus uptake ($mgl^{-1}$), $K_1$: background light attenuation coefficient ($m^{-1}$), $K_{nit}$: half-saturation constant for oxygen limitation of nitrification ($mgl^{-1}$), $\Psi$: strength of the ammonium preference ($mgl^{-1}$), $\theta_m$: temperature adjustment for phytoplankton mortality rate, $\theta_r$: temperature adjustment for phytoplankton respiration rate, $\theta_{mn}$: temperature adjustment for organic nitrogen mineralization rate, $\theta_{mp}$: temperature adjustment for organic phosphorus mineralization rate.*j*: *Cy*, *Diat*, *Chl* for taxonomic approach and *j*: *C*, *D*, *F*, *H1*, *J*, *M*, *P* for functional group approach.

| Parameter | Unit | Range | Initial value | Optimal value | Parameter | Unit | Range | Initial value | Optimal value |
|---|---|---|---|---|---|---|---|---|---|
| **Taxonomical group approach** | | | | | | | | | |
| $k_{Cy,growth}$ | 1/d | 0.1–3.3 | 0.20 | 0.22 | $K_1$ | 1/m | 0.25–5.0 | 2.00 | 2.14 |
| $k_{Diat,growth}$ | 1/d | 0.2–3.6 | 0.66 | 1.00 | $K_{nit}$ | mg/L | $7.0E^{-4}$-2.0 | 0.12 | 0.19 |
| $k_{Chl,growth}$ | 1/d | 0.2–3.6 | 0.76 | 0.85 | $\theta_m$ | – | 1.00–1.09 | 1.02 | 1.00 |
| $k_{Diat,death}$ | 1/d | 0.03–0.59 | 0.15 | 0.48 | $\theta_r$ | – | 1.00–1.09 | 1.05 | 1.08 |
| $k_{Chl,death}$ | 1/d | 0.03–0.46 | 0.10 | 0.15 | $\theta_{mn}$ | – | 1.02–1.12 | 1.08 | 0.96 |
| $I_{optCy}$ | $w/m^2$ | 32–143 | 53 | 79 | $\theta_{mp}$ | – | 1.00–1.12 | 1.08 | 0.99 |
| $I_{optChl}$ | $w/m^2$ | 40–116 | 47 | 48 | $\Psi$ | – | | 0.03 | 0.01 |
| $K_{PCy}$ | mg/L | $3.0E^{-4}$–$4.0E^{-2}$ | $2.0E^{-3}$ | $2.0E^{-4}$ | | | | | |
| $K_{PDiat}$ | mg/L | $1.0E^{-4}$–$4.0E^{-2}$ | 0.03 | 0.30 | | | | | |
| $K_{PChl}$ | mg/L | $1.0E^{-4}$–$4.0E^{-2}$ | 0.03 | $9.0E^{-4}$ | | | | | |
| **Functional group approach** | | | | | | | | | |
| $k_{C,growth}$ | 1/d | 0.2–3.6 | 1.24 | 1.39 | $K_{Pj}$ | mg/L | $1.0E^{-4}$–$4.0E^{-2}$ | $1.0E^{-4}$ | $2.0E^{-4}$ |
| $k_{D,growth}$ | 1/d | 0.2–3.6 | 0.66 | 0.56 | $K_{PM}$ | mg/L | $3.0E^{-4}$–$4.0E^{-1}$ | $1.4E^{-3}$ | $1.0E^{-4}$ |
| $k_{F,growth}$ | 1/d | 0.2–3.6 | 0.99 | 1.72 | $K_{PP}$ | mg/L | $1.0E^{-4}$–$4.0E^{-2}$ | 0.01 | $1.0E^{-4}$ |
| $k_{H1,growth}$ | 1/d | 0.1–3.3 | 0.50 | 0.69 | $I_{optC}$ | $w/m^2$ | 7–64 | 5 | 5 |
| $k_{J,growth}$ | 1/d | 0.2–3.6 | 1.07 | 0.63 | $I_{optD}$ | $w/m^2$ | 7–64 | 14 | 16 |
| $k_{M,growth}$ | 1/d | 0.1–3.3 | 0.32 | 0.56 | $I_{optF}$ | $w/m^2$ | 7–64 | 17 | 25 |
| $k_{P,growth}$ | 1/d | 0.2–3.6 | 0.22 | 0.17 | $I_{optH1}$ | $w/m^2$ | 32–197 | 49 | 81 |
| $k_{C,death}$ | 1/d | 0.03–0.59 | 0.49 | 0.43 | $I_{optJ}$ | $w/m^2$ | 32–197 | 102 | 143 |
| $k_{D,death}$ | 1/d | 0.03–0.59 | 0.44 | 0.44 | $I_{optM}$ | $w/m^2$ | 32–197 | 106 | 159 |
| $k_{F,death}$ | 1/d | 0.03–0.46 | 0.03 | 0.03 | $I_{optP}$ | $w/m^2$ | 7–117 | 38 | 57 |
| $k_{H1,death}$ | 1/d | 0.03–0.12 | 0.05 | $1.0E^{-4}$ | $K_1$ | 1/m | 0.25–5.0 | 1.26 | 0.97 |
| $k_{J,death}$ | 1/d | 0.03–0.46 | 0.44 | 0.13 | $K_{nit}$ | mg/L | $7.0E^{-4}$-2.0 | 0.051 | 0.047 |
| $k_{M,death}$ | 1/d | 0.03–0.12 | 0.10 | 0.20 | $\theta_m$ | – | 1.00–1.09 | 1.042 | 1.061 |
| $k_{P,death}$ | 1/d | 0.03–0.46 | 0.09 | 0.08 | $\theta_r$ | – | 1.00–1.09 | 1.080 | 1.098 |
| $K_{PC}$ | mg/L | $1.0E^{-4}$–$4.0E^{-2}$ | 0.09 | 0.08 | $\theta_{mn}$ | – | 1.02–1.12 | 1.020 | 1.000 |
| $K_{PD}$ | mg/L | $1.0E^{-4}$–$4.0E^{-2}$ | 0.01 | $1.0E^{-3}$ | $\theta_{mp}$ | – | 1.00–1.12 | 1.020 | 1.023 |
| $K_{PF}$ | mg/L | $1.0E^{-4}$–$4.0E^{-2}$ | 0.30 | 0.80 | $\Psi$ | – | | 0.057 | 0.246 |
| $K_{PH1}$ | mg/L | $3.0E^{-4}$–$4.0E^{-1}$ | 0.17 | 0.44 | | | | | |

References: Mechling and Kilham (1982), Reynolds (1984), Asaeda and Van Bon (1997), Fasham (1993), Bruce et al. (2006), Cerco and Cole (1994), Omlin et al. (2001b), Priyantha et al. (1997), Wetzel (2001), Bonnet and Poulin (2002), Chen et al. (2002), Hongping and Jianyi (2002), Romero et al. (2004), Arhonditsis and Brett (2005a), Makler-Pick et al. (2011), Rigosi et al. (2011).

even when collected data show an important dispersion. The timing of the peak is in good agreement with the observed data (Fig. 5).

In the functional group-based model, all phytoplankton variables show good agreement with the observed data (Table 9). As it is shown in Fig. 6, the model always reproduces the dominant group of the phytoplankton community along the time horizon. It can be seen that the observed data patterns are simpler (in terms of number of peaks) when classified within functional groups, showing less dispersion (compare Figs. 5 and 6).

Prediction of cyanobacteria concentration included in group H1 (mainly *Dolichospermum circinalis*) and group M (mainly *Microcystis* spp.) is in satisfactory agreement (Table 9). Table 10 shows the differences between mean predicted output value and mean observed data for the period of the main biomass peak in the year. These differences, for groups H1 and M, are 0.90 and 18.54%, respectively.

Because of its implication in human and ecosystem health, one of the main concerns in water quality modeling is to find a better representation of cyanobacteria population dynamics. The taxonomic group-based model we propose attains a good representation of cyanobacteria blooms, with one state variable. The functional group-based model, which describes dominant cyanobacteria species with two state variables (M and H1 concentration) provides a better ecological representation. This model is able to capture the different preferences of group *M* and group *H1* species for temperature, light and nutrients. Numerical results provide an optimal growth temperature value of 30 °C for group *M* and 23.8 °C for *group H1*, *respectively*. These results are in agreement with optimal growth temperatures for *Microcystis* (dominant within group M), between 30 and 35 °C (Chu et al., 2007; Imai et al., 2009) and *Dolichospermum* (dominant within group H1) optimal-growth temperatures are below 25 °C (Bormans et al., 2005). During the study period, water temperature was optimum until the end of

**Table 9**
**Calibration**: medium (*ME*), relative error (*RE*) and index of agreement (*d*) of the main model variables for taxonomic and functional group models.

| | Mean error (mg/l) | Relative error (%) | *d* (dimensionless) |
|---|---|---|---|
| **Taxonomic model** | | | |
| Cyanobacteria | −0.045 | 39.5 | 0.91 |
| Diatoms | −0.086 | 117.0 | 0.53 |
| Chlorophyta | 0.224 | 56.6 | 0.77 |
| Nitrate | 0.035 | 13.9 | 0.61 |
| Phosphate | −0.017 | 41.8 | 0.43 |
| Dissolved oxygen | 0.730 | 47.9 | 0.81 |
| **Functional groups model** | | | |
| C | 0.002 | 27.7 | 0.99 |
| D | 0.005 | 54.6 | 0.94 |
| F | 0.072 | 43.3 | 0.90 |
| H1 | 0.057 | 51.6 | 0.89 |
| J | 0.052 | 67.4 | 0.80 |
| M | 0.002 | 46.7 | 0.90 |
| P | 0.001 | 45.3 | 0.79 |
| Nitrate | 0.021 | 13.4 | 0.22 |
| Phosphate | 0.005 | 22.0 | 0.89 |
| Dissolved oxygen | −0.210 | 32.2 | 0.81 |

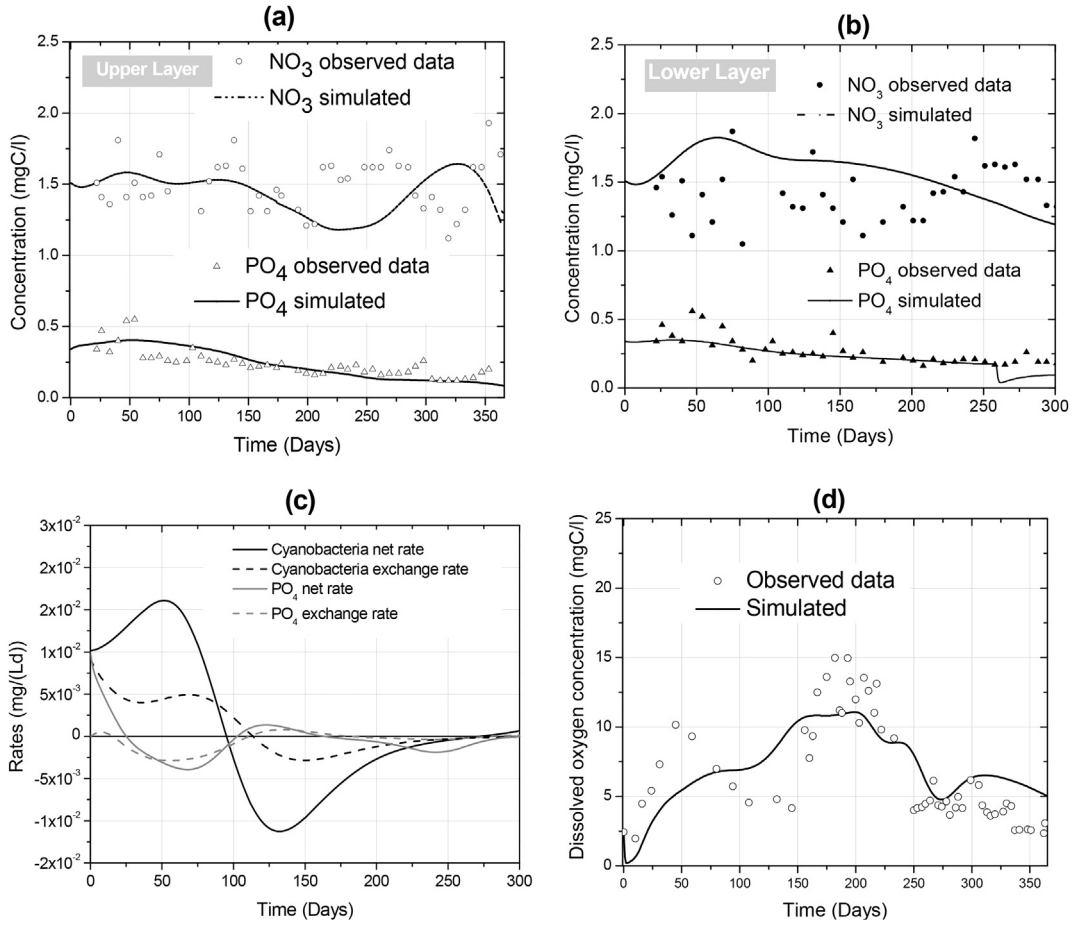


**Fig. 7.** Calibration. Time series for inorganic nutrients of the upper layer (a), lower layer (b), exchange and net generation rates for cyanobacteria and SRP (c) and dissolved oxygen (d) for functional group approach.

**Table 10**
Mean biomass concentration for each functional group during bloom period.

| | Bloom period | Mean observed values (mg/l) | Mean simulated values (mg/l) |
|---|---|---|---|
| Group C | 24/06–17/08 | 0.269 | 0.298 |
| Group D | 20/08–11/11 | 0.251 | 0.241 |
| Group F | 26/04–17/08 | 0.459 | 0.432 |
| Group H1 | 01/01–01/04 | 0.342 | 0.345 |
| Group J | 01/01–01/04 | 0.542 | 0.448 |
| Group M | 01/01–07/04 | 0.151 | 0.123 |
| Group P | 19/02–06/05 | 0.171 | 0.170 |

February for *D. circinalis*, whereas *Microcystis* growth was slightly limited during the bloom periods because water temperature in Paso de las Piedras was not at its optimal value. It is known that *Microcystis* has greater requirements of light than *Dolichospermum* (Robarts and Zohary, 1992) and this is well represented by the optimal values obtained in the calibration process of the functional group-based model.

Another important feature that can be represented by the functional group-based model is the different dynamics of phosphorus uptake by both functional groups describing cyanobacteria. Through the values obtained in the calibration for the parameters involved in phosphorus uptake (Table 8), the functional group-based model represents well the fact that *Microcystis* (group M) grows better than *Dolichospermum* (group H1) in non-limited phosphorus conditions (Nalewajko and Murphy, 2001). Model limiting functions (Eqs. A.2-A.5) can take values between 0 and 1. Values closer to zero indicate an important growth limitation. During the calibration period, the phosphorus limiting function for group M is always close to 1 (no limitation) whereas for group H1 it is lower than 0.7, indicating limitation by nutrients. These results are in agreement with Reynolds (1984, 1997), who stated that phytoplankton distribution among different types of habitats (based on the accessibility of light and nutrient resources) coincides substantially with algae classification based on their morphologies.

During the studied period, chlorophytes were the most diverse phytoplankton group, represented by 87 *taxa*. The taxonomic group-based model, which requires one state variable for chlorophyte concentration, predicts the main biomass peak (Fig. 5) but fails to correctly predict the chlorophytes succession pattern, as demonstrated by the goodness-of-fit statistics (Table 9). On the other hand, the functional group-based model is able to predict the switch in the dominating groups of green algae throughout the

year, mainly due to the inclusion of three different state variables to describe chlorophyte concentration (F, J and P), which have different requirements for growth (Fig. 6). The difference between simulated and observed mean biomass value of P, F and J groups during the main peak periods is 0.58%, 5.88% and 17.34%, respectively, also indicating a good model performance. Several species of the coenobial genera *Coelastrum,* along with other colonial chlorococcales (group J) developed a summer bloom. It is well known that these organisms have high light requirements (Becker et al., 2010), which is in good agreement with the optimal calibrated parameter value, $I_{optJ}$ (optimal light intensity for group J growth, Table 8). Furthermore, as also observed in other nutrient-rich environments (Tucker and Llyod, 1984; Kim and Boo, 2001), a winter bloom of green algae is developed by organisms of group F, mainly composed of *Dictyosphaerium pulchellum* and *D. ehrermbergianum*. This biomass peak cannot be captured by the taxonomic group-based model because of the difference between the growth model parameter values obtained in calibration for Chlorophytes concentration and those that represent light, temperature and nutrient requirements of species aggregated in group F. In particular, group F tolerates mild light intensities (Table 7) with an optimal value of 48 w/m$^2$in$I_{optJ}$.Diatoms and chlorophytes included in group P (mainly *Aulacoseira, Closterium and Staurastrum* species, Table 3) are filter-clogging algae, not well represented by the taxonomic group-based model. In this model, *Alulacoseira* spp are included in the state variable diatom concentration. However, these organisms have very different growth requirements than the other two dominant diatoms in Paso de las Piedras Reservoir (*Cyclotella meneghiniana* and *Stephanodiscus* sp.). These last ones have higher optimal temperatures and light for growth and lower settling rates (Table 8). Statistical measures for the functional group-based model show a good agreement for group P ($ME = 0.001$ mg/L, $RE = 45.3\%$, $d = 0.79$). The functional group-based model also improves the representation of winter–spring peaks of groups C and D, which include the most conspicuous centric diatoms of Paso de las Piedras Reservoir (Fig. 6, Tables 9 and 10). The functional group-based model captures the three annual peaks of diatoms. The first peak is in summer, represented by group P (mainly *Aulacoseira*), while the other two biomass peaks take place in the cold period, represented by group C (*Cyclotella meneghiniana*) in early winter, and group D (*Stephanodiscus* sp.) between late winter and early spring.

Regarding nutrient concentrations, Table 9 and Fig. 7 show that *RE* and*ME* for nitrate concentration in the functional group-based model presents a slight improvement as compared to the taxonomic group-based model (Table 9). Also the mean annual nitrate concentration obtained with the functional group-based model shows an improvement, with 1.43% variation with respect to observed values, whereas the taxonomic model shows 2.39% variation (Fig. 7). Table 9 and Fig. 7 also show phosphate goodness-of-fit statistics of the functional group-based model, showing very good agreement with collected data and an important improvement, as compared to the taxonomic group-based approach. The variation of the mean annual phosphate concentration with respect to observed data for the taxonomic model and the functional group model are 6.85% and 1.90%, respectively. As in most freshwater ecosystems, phosphorus is the limiting nutrient of the primary productivity in Paso de las Piedras. The reason for this assumption is the increment of nitrogen concentration within the water body due to the presence of cyanobacteria with heterocysts that can fix atmospheric nitrogen (Vollenweider, 1975; Schindler et al., 2008). Therefore, the accurate tuning of phosphate concentrations is an important issue in lakes and reservoir models. Fig. 7(b) shows a good fit for inorganic nutrients concentration profiles and observed data for the lower layer of the water column. A comparison of the exchange rates between layers and the generation/consumption rates (net rates) for the model variables shows that the vertical spatial resolution is required since the absolute value of the exchange rates are lower than the generation rates most of the time (Fig. 7(c)).

Finally, dissolved oxygen concentrations predicted with the functional group-based model also have a better fit than those obtained with the taxonomic group-based approach (Table 9 and Fig. 7(d)), with variations of annual mean concentrations of 3.06% and 10.64%, respectively.

Additionally, monthly mean residual values for phytoplankton variables of the taxonomic and functional group-based models are shown in Appendix D (Figures D.1 and D.2, respectively). As it is observed in Figure D.2, residual values are closer to zero, showing that the functional group-based model provides a better description of the phytoplankton community behavior.

After calibration, we carry out model validation with an independent data set collected during the 2005 summer-autumn bloom. Numerical results and collected data are shown in Figure E.1, from Appendix E. It can be seen that cyanobacteria community is more accurately represented by the functional group-based model than the taxonomic one. Statistical diagnostic measures of model performance for the mean of the sampling stations for group M and group H1 (Figure E.1) concentrations are $ME = -5.7 \times 10^{-4}$ mg/L, $RE = 15.50\%$,$d = 0.99$ and $ME = 0.041$ mg/L, $RE = 69.67\%$,$d = 0.79$, respectively. These values indicate a considerable improvement with respect to the taxonomic group-based model, which presents poor statistical values ($ME = -0.56$ mg/L, $RE = 635.4\%$,$d = 12$)for cyanobacteria concentration (Figure E.1). Also, FigureE.1shows an adequate representation of desmids and diatoms species included in group P, which causes filter blocking in the potabilization process during blooms. The functional group-based model can provide information for the determination of additional measures that must be taken in the water purification process according to the species that constitute the blooms. That is in line with the issue that morphological group-based models better represent environmental conditions as compared to phylogenetic group-based models, giving a better description of the ecosystem functioning (Kruk et al., 2011).

**Table 11**
Mean annual values for phosphate, total phytoplankton and individual functional groups biomass concentrations for different nutrient scenarios. In brackets: percentage of total biomass of each group. *O*: oligotrophic-metrophic, *E*: eutrophic and *H*: hipertrophic.

| | $PO_4$ (μg/l) | Total phytoplankton (mg/l) | Group C (mgC/l) | Group D (mgC/l) | Group F (mgC/l) | Group $H_1$ (mgC/l) | Group J (mgC/l) | Group M (mgC/l) | Group P (mgC/l) |
|---|---|---|---|---|---|---|---|---|---|
| **O** | 2.8 | 0.18 | 0.012 (0.7%) | 0.026 (14.4%) | 0.009 (4.9%) | 0.002 (1.2%) | 0.030 (16.8%) | 0.017 (9.6%) | **0.095 (52.4%)** |
| | 7.0 | 0.25 | 0.014 (0.6%) | 0.0361 (14.6%) | 0.009 (3.7%) | 0.002 (1.0%) | 0.072 (29.3%) | 0.030 (12.3%) | **0.100 (38.7%)** |
| **E** | 38.8 | 0.34 | 0.020 (0.6%) | 0.064 (19.0%) | 0.011 (3.1%) | 0.004 (1.1%) | **0.118 (35.0%)** | 0.042 (12.6%) | 0.100 (28.7%) |
| | 122.4 | 0.36 | 0.051 (1.4%) | 0.064 (18.1%) | 0.017 (4.8%) | 0.009 (2.4%) | **0.121 (33.9%)** | 0.043 (12.2%) | 0.097 (27.2%) |
| **H** | 200.5 | 0.63 | 0.048 (7.6%) | 0.064 (10.2%) | **0.158 (25.1%)** | 0.098 (15.6%) | 0.121 (19.3%) | 0.043 (6.9%) | 0.100 (15.4%) |
| | 241.8 | 0.95 | 0.035 (3.6%) | 0.064 (6.7%) | 0.065 (6.8%) | **0.529 (55.5%)** | 0.121 (12.7%) | 0.043 (4.5%) | 0.097 (10.1%) |

Bold type indicate dominant functional group.

### 4.3. Analysis of alternative trophic state scenarios

The trophic state of Paso de las Piedras Reservoir has already been studied in previous work (Intartaglia and Sala, 1989; Fernández et al., 2009). Based on chlorophyll a concentration and turbidity data, the reservoir was included within the eutrophic category. However, according to total phosphorus concentration this water body is within the hypereutrophic state.

To study phytoplankton sensitivity to changes in phosphorus concentration, we run six different trophic scenarios for phosphate concentration, corresponding to oligo-mesotrophic (2.8 and 7.0 SRP μg/L mean annual concentration), eutrophic (38.8 and 122.4 SRP μg/L mean annual concentration) and hypereutrophic (200.5 and 241.8 SRP μg/L mean annual concentration) states, respectively. These trophic scenarios are achieved varying phosphorus concentration in the tributaries. Table 11 shows, for each trophic scenario, the mean annual phosphate within the water body, total phytoplankton and functional group abundance, as well as the percentage of total biomass corresponding to each group. Numerical results (Fig. 8 and Table 11) show that, as limiting nutrient concentration increases, cyanobacteria concentration increases as well. For the first scenario of eutrophic condition (38.8 μg/L) the

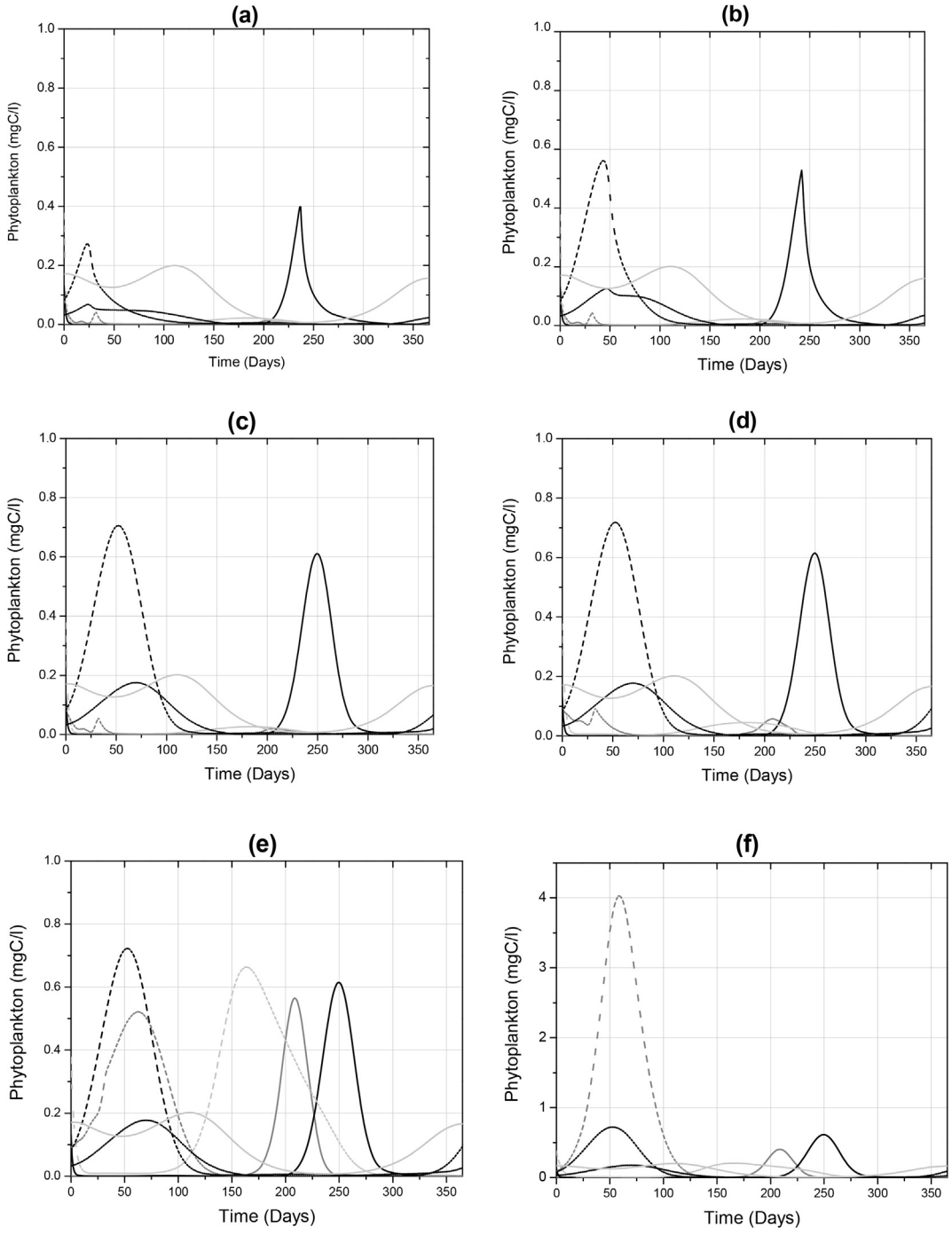


**Fig. 8.** Succession phytoplankton patterns for oligo-mesotrophic (a and b), eutrophic (c and d) and hypereutrophic (e and f) scenarios.

abundance of group M increases up to a certain value and remains constant with rising phosphate concentration. On the other hand, cyanobacteria concentration within group H1 remains low until hypereutrophic conditions are reached. At this point, it becomes completely dominant over group M *(Microcystis* spp) and over the other functional groups. Nutrient loading and water temperature are two main driving forces for cyanobacteria development. The functional group-based model we propose in this paper predicts that group H1 is more sensitive to phosphorus increase than group M, in agreement with a recent experimental study carried out over more than 100 U.S. lakes (Rigosi et al., 2014). Group C biomass shows an increase under hypereutrophic conditions, with the largest increase at actual phosphate concentration (200.5 μg/L), while group D achieves the highest concentration in eutrophic scenarios and keeps these values in hypereutrophic conditions. Mean annual biomass of group P remains constant throughout the phosphorus concentration gradient, representing over 50% of total phytoplankton biomass under oligotrophic conditions to 10% in the last hypertrophic scenario (Table 11). Phosphate concentration observed during the study period (200.5 μg/L) supports the highest biomass concentration of group F, with 25% of mean annual total biomass. Colonial chlorococcales of group J reaches the highest concentration at the second scenario of eutrophic condition and remains constant under hypereutrophic conditions.

## 5. Conclusions

In this paper we have assessed the performance of two mechanistic water quality models with different approaches for the description of phytoplankton community in a non-stratified water body. These approaches aggregate phytoplankton species according to taxonomic or functional group criteria (based on Reynolds' classification) and both models are formulated in the same physical and numerical framework.

The parameter estimation problems subject to differential algebraic constraints have been solved within an equation oriented framework in gPROMS and the goodness of fit of both models has been assessed, showing a better performance of the functional group-based model. This is closely related to the way phytoplankton data are grouped in the different approaches. The functional group classification provides simpler patterns for phytoplankton concentration, with low observed data dispersion. Furthermore, in both models, properties such as the affinity for different nutrients at different external concentrations, silica requirements, light necessities and tolerance, etc. are, in part, determined by parameter values selected in the calibration process. These parameter values are more related to functional and morphological properties of each species than by phylogeny. An optimal set of parameter values is more representative of the species within a functional group than the parameters of taxonomic groups which include species which may have very different growth requirements. .

Although the functional group-based model implies a 38% increase in the total number of differential equations, the solution approach proved to be quite efficient and the additional computational cost is acceptable (275 s against 27.6 s for solving the entire parameter estimation problem).

Finally, we can conclude that mathematical models are important tools for planning and decision making in different processes, on the short and long term. In the case of water reservoir management, ecological models are being increasingly used in the identification of possible problems and in decision making processes. As future work, the functional group-based model is being extended to include zooplankton and fish dynamics as it has been done with the taxonomic group-based model (Estrada et al., 2011). The extended model will provide a reliable basis for the formulation of an optimal control problem to plan restoration policies, evaluate their effects on water quality and the economic feasibility of their implementation.

## Acknowledgments

The authors gratefully acknowledge financial support from the National Research Council (CONICET) (Grant number: PIP 11220110101078), Universidad Nacional del Sur (Grant number 24/M125) and ANPCyT (Grant number: PICT 2012-2469), Argentina.

## Appendix A. Generation/consumption terms for mass balance equations (Table 1, Eqs (1) and (2)) of Paso de las Piedras Reservoir water quality model. $i$ = upper ($U$) and lower layer ($L$). For taxonomic approach $j$ = *Cy*, *Chl*, *Diat* and for functional group approach $j$ = *C*, *D*, *F*, *H*1, *J*, *M*,*P*.

**Phytoplankton population change**

$$r_{ij} = R_{growth,ij} - R_{resp,ij} - R_{death,ij} - R_{settling,\ ij} \tag{A.1}$$

Specific phytoplankton growth rate $R_{growth,ij} = k_{growth,i} f_j(T_i) f_j(I_i) f_j(N_i) C_{ij}$ (A.2)

Temperature limitation $f_j(T_i) = \frac{T_i}{T_{opt_j}} exp\left(1 - \frac{T_i}{T_{opt_j}}\right)$ (A.3)

Nutrient limitation $f_j(N_i) = \begin{cases} min\left[\frac{C_{i,PO_4}}{C_{i,PO_4} + K_{Pj}}, \frac{C_{i,Si}}{C_{i,S_i} + K_{Sij}}\right] j = D_{iat} \text{ or } j = C \\ \frac{C_{i,PO_4}}{C_{i,PO_4} + K_{Pj}} \quad j = Cy, Chl \text{ or } J = D, F, H1, J, M, P \end{cases}$ (A.4)

Light limitation $f_j(I_i) = \frac{I_{O_i}}{I_{opt_j}} exp\left(1 - \frac{I_{O_i}}{I_{opt_j}}\right)$

$I_{0_i} = \frac{I[1 - exp(-K_e \Delta D_i)]}{K_e \Delta D_i}, \quad K_e = K_1 + K_2 \frac{\sum C_{ij}}{cchl}$ (A.5)

(*continued*)

Respiration $R_{resp,ij} = k_{resp,j}\theta_r^{(T-20)}C_{ij}$ (A.6)

Death $R_{death,ij} = k_{death,j}\theta_m^{(T-20)}C_{ij}$ (A.7)

Settling $R_{settling,ij} = k_{settling,j}\dfrac{C_{ij}}{h_i}$ (A.8)

**Rate of change of nitrogen cycle compounds concentration**

$$r_{NH_4,i} = \begin{cases} -R_{uptake,i,NH_4} - R_{nit,i,NH_4} + R_{death,i,NH_4} + R_{miner,i,ON} & i = U \\ -R_{uptake,i,NH_4} - R_{nit,i,NH_4} + R_{death,i,NH_4} + R_{miner,i,ON} + R_{sed,i,NH_4} & i = L \end{cases} \quad \text{(A.9)}$$

$$r_{NO_3,i} = -R_{NO_3,uptake,i} + R_{NH_4,nit,i} - R_{NO_3,denit,i} \quad \text{(A.10)}$$

$$r_{ON,i} = \begin{cases} R_{death,i,ON} + R_{miner,i,ON} - R_{ON,i,settling} & i = U \\ R_{death,i,ON} + R_{miner,i,ON} - R_{ON,settling} + R_{ON,U,settling} & i = L \end{cases} \quad \text{(A.11)}$$

Phytoplankton $NH_4$ uptake $R_{uptake,i,NH_4} = \sum_j \left(\alpha_{nc}R_{growth,j}P_{NH_4}\right)$ (A.12)

$NH_4$ preference factor $P_{NH_4} = 1 - exp(\Psi_j C_{i,NH_4})$ (A.13)

$NH_4$ release by phytoplankton death $R_{death,i,NH_4} = \sum_j \left(C_{ij}k_{death,j}\alpha_{nc}(1 - f_{ON})\right)$ (A.14)

Nitrification rate $R_{nit,i,NH_4} = k_{nit}\theta_{nit}^{(T-20)}\dfrac{C_{i,DO}}{K_{nit} + C_{i,DO}}C_{i,NH_4}$ (A.15)

ON mineralization rate $R_{miner,i,ON} = k_{mn}\theta_{mn}^{(T-20)}\dfrac{\sum_j C_{ij}}{K_{mpc} + \sum_j C_{ij}}C_{i,ON}$ (A.16)

$NH_4$ release from sediments $R_{sed,i,NH_4} = S_N\left(1 - \dfrac{C_{L,DO}}{K_{DOS} + C_{L,DO}}\right)A$ (A.17)

Phytoplankton $NO_3$ uptake $R_{uptake,i,NO_3} = \sum_j \left(\alpha_{nc}R_{growth,j}(1 - P_{NH_4})\right)$ (A.18)

Denitrification rate $R_{denit,i,NO_3} = k_{denit}\theta_{denit}^{(T-20)}\dfrac{K_{denit}}{K_{denit} + C_{i,DO}}C_{i,NO_3}$ (A.19)

ON release by phytoplankton death $R_{uptake,i,ON} = \sum_j \left(C_{ij}k_{death,j}\alpha_{nc}(f_{ON})\right)$ (A.20)

ON settling rate $R_{,,} = \dfrac{k_{setlling}}{h_i}C_{i,ON}$ (A.21)

**Rate of change of phosphorus cycle compounds concentration**

$$r_{i,PO_4,} = \begin{cases} -R_{uptake,i,PO_4} + R_{death,i,PO_4} + R_{miner,i,OP} & i = U \\ -R_{uptake,i,PO_4} + R_{death,i,PO_4} + R_{miner,i,OP} + R_{sed,i,PO_4} & i = L \end{cases} \quad \text{(A.22)}$$

$$r_{i,OP} = \begin{cases} R_{death,i,OP} + R_{miner,i,OP} - R_{OP,i,settling} & i = U \\ R_{death,i,OP} + R_{miner,i,OP} - R_{OP,i,settling} + R_{OP,U,settling} & i = L \end{cases} \quad \text{(A.23)}$$

Phytoplankton $PO_4$ uptake $R_{uptake,i,PO_4} = \sum_J \left(\alpha_{pc}R_{growth,j}\right)$ (A.24)

$PO_4$ release by phytoplankton death $R_{death,i,PO_4} = \sum_j \left(C_{ij}k_{death,j}\alpha_{pc}(1 - f_{OP})\right)$ (A.25)

(*continued on next page*)

(*continued*)

$PO_4$ release from sediments $R_{sed,L,PO_4} = S_P\left(1 - \frac{C_{L,DO}}{K_{DOS} + C_{L,DO}}\right)A$ (A.26)

OP release by phytoplankton death $R_{uptake,i,OP,} = \sum_j \left(C_{ij} k_{death,j} \alpha_{pc} (f_{OP})\right)$ (A.27)

OP mineralization rate $R_{miner,i,OP} = k_{mp}\theta_{mp}^{(T-20)} \frac{\sum_j C_{ij}}{K_{mpc} + \sum_j C_{ij}} C_{i,OP}$ (A.28)

OP settling rate $R_{i,OP} = \frac{k_{setlling}}{h_i} C_{i,OP}$ (A.29)

**Rate of change of dissolved oxygen concentration**

$$r_{i,DO} = \begin{cases} R_{reai,i,DO} - R_{nit,i,DO} + R_{resp/photo,i,DO} - R_{oxid,i,BDO} & i = U \\ -R_{nit,i,DO} + R_{resp/photo,\ i,DO} - R_{bod,i,DO} - R_{oxid,i,BDO} & i = L \end{cases} \quad \text{(A.30)}$$

Re – aeration rate $R_{reair,U,DO} = \frac{k_a \theta_a^{(T-20)}}{h_U}(C^* - C_{U,DO})$ (A.31)

Saturated dissolved oxygen $C^* = 16.5 - \frac{8}{12}T$ (A.32)

DO consumed in nitrification process $R_{nit,i,DO} = k_{nit}\theta_{nit}^{(T-20)} \frac{C_{i,DO}}{K_{nit} + C_{i,DO}} C_{i,NH_4} \alpha_{on}$ (A.33)

Net production of oxygen by respiration/photosynthesis

$$R_{resp/phot,i,DO} = \left(\sum_j \left(R_{growth,ij} - R_{resp,ij}\right)\right)\alpha_{oc} \quad \text{(A.34)}$$

Sediment oxygen demand $R_{sed,i,DO} = \frac{k_{sod}\theta_{sod}^{(T-20)}}{h_L} \frac{C_{L,DO}}{K_{sod} + C_{L,DO}}$ (A.35)

**Rate of change of biochemical oxygen demand concentration**

$r_{BOD,i} = R_{death,i,BOD} - R_{oxid,i,BOD} - R_{settling,i,BOD}$ (A.36)

BOD generation by phytoplankton death $R_{death,i,BOD} = \sum_j \left(R_{death,j}\alpha_{oc}\right)$ (A.37)

DO for organic matter oxidation $R_{oxid,i,BOD} = k_{bod}\theta_{bod}^{(T-20)} \frac{C_{i,DO}}{K_{bod} + C_{i,DO}} C_{i,BOD}$ (A.38)

BOD settling rate $R_{settling,i,BOD} = \frac{k_{setlling,BOD}}{h_i} C_{i,BOD}$ (A.39)

## Appendix B. Parameters of Paso de las Piedras Reservoir water quality model.

| Parameter | Unit | Description | Value |
|---|---|---|---|
| **Taxonomical approach** | | | |
| $k_{Cy,resp}$ | 1/d | Respiration rate for cyanobacteria | 0.05 |
| $k_{Diat,resp}$ | 1/d | Respiration rate for diatoms | 0.48 |
| $k_{Chl,resp}$ | 1/d | Respiration rate for chlorophytes | 0.42 |
| $k_{Cy,settling}$ | m/d | Settling rate for cyanobacteria | 0.15 |
| $k_{Diat,settling}$ | m/d | Settling rate for diatoms | 0.20 |
| $k_{Chl,settling}$ | m/d | Settling rate for chlorophytes | 0.15 |
| $T_{optCy}$ | °C | Optimal temperature for cyanobacteria | 30.0 |
| $T_{optDiat}$ | °C | Optimal temperature for diatoms | 17.7 |
| $T_{optChl}$ | °C | Optimal temperature for chlorophytes | 20.0 |
| $I_{optChl}$ | $w/m^2$ | Optimal light intensity for Chlorophytes | 43.48 |

(*continued*)

| Parameter | Unit | Description | Value |
|---|---|---|---|
| **Taxonomical approach** | | | |
| $K_{PCy}$ | mg/L | Half-sat. const. for P uptake by cyanobacteria | 0.0002 |
| $K_{PDiat}$ | mg/L | Half-sat. const. for P uptake by diatoms | 0.3 |
| $K_{PChl}$ | mg/L | Half-sat. const. for P uptake by chlorophytes | 0.0009 |
| $K_{Sij}$ | mg/L | Half-sat. const. for Si uptake by diatoms | 0.0053 |
| **Functional approach** | | | |
| $k_{C,resp}$ | 1/d | Respiration rate for functional group C | 0.19 |
| $k_{D,resp}$ | 1/d | Respiration rate for functional group D | 0.19 |
| $k_{F,resp}$ | 1/d | Respiration rate for functional group F | 0.50 |
| $k_{H1,resp}$ | 1/d | Respiration rate for functional group H1 | 0.08 |
| $k_{J,resp}$ | 1/d | Respiration rate for functional group J | 0.03 |
| $k_{M,resp}$ | 1/d | Respiration rate for functional group M | 0.06 |
| $k_{P,resp}$ | 1/d | Respiration rate for functional group P | 0.02 |
| $k_{C,settling}$ | m/d | Settling rate for functional group C | 0.16 |
| $k_{D,settling}$ | m/d | Settling rate for functional group D | 0.32 |
| $k_{F,settling}$ | m/d | Settling rate for functional group F | 0.06 |
| $k_{H1,settling}$ | m/d | Settling rate for functional group H1 | 0.50 |
| $k_{J,settling}$ | m/d | Settling rate for functional group J | 0.80 |
| $k_{M,settling}$ | m/d | Settling rate for functional group M | 0.02 |
| $k_{P,settling}$ | m/d | Settling rate for functional group P | 0.08 |
| $T_{optC}$ | °C | Optimal temperature for functional group C | 14.6 |
| $T_{optD}$ | °C | Optimal temperature for functional group D | 6.0 |
| $T_{optF}$ | °C | Optimal temperature for functional group F | 26.5 |
| $T_{optH1}$ | °C | Optimal temperature for functional group H1 | 23.8 |
| $T_{optJ}$ | °C | Optimal temperature for functional group J | 21.4 |
| $T_{optM}$ | °C | Optimal temperature for functional group M | 30.0 |
| $T_{optP}$ | °C | Optimal temperature for functional group P | 18.2 |
| $K_{Sij}$ | mg/L | Half-sat. const. for Si uptake by functional group C | 0.08 |
| **General** | | | |
| $k_{nit}$ | 1/d | Nitrification rate | 0.09 |
| $k_{denit}$ | 1/d | Denitrification rate | 0.001 |
| $k_{mn}$ | 1/d | Organic nitrogen mineralization rate | 0.032 |
| $k_{mp}$ | 1/d | Organic phosphorus mineralization rate | 0.02 |
| $k_{bod}$ | 1/d | BOD deoxygenation rate | 0.50 |
| $k_{sod}$ | 1/d | Sediment oxygen demand rate | 0.65 |
| $S_N$ | $mg/m^2/d$ | Release rate of ammonium from the sediment | 0.40 |
| $S_P$ | $mg/m^2/d$ | Release rate of phosphate from the sediment | 0.0013 |
| $K_{denit}$ | mg/L | Half-sat. const. for oxygen limitation of denitrification | 0.2 |
| $K_{bod}$ | mg/L | Half-sat. const. for oxygen limitation of BOD oxidation | 0.5 |
| $K_{sod}$ | mg/L | Half-sat. const. for sediment oxygen demand | 0.4 |
| $K_{mpc}$ | mg/L | Half-sat. const. for phytoplankton limitation | 1.0 |
| $K_{DOS}$ | mg/L | Half-sat. const. for nutrient sediment fluxes | 0.4 |
| $k_{ON,settling}$ | m/d | Settling velocity for organic nitrogen | 0.03 |
| $k_{OP,settling}$ | m/d | Settling velocity for organic phosphorus | 0.03 |
| $k_{bod,settling}$ | m/d | Settling velocity for BOD | 0.03 |
| $\theta_{nit}$ | – | Temp. adjustment for nitrification rate | 1.080 |
| $\theta_{denit}$ | – | Temp. adjustment for denitrification rate | 1.080 |
| $\theta_N$ | – | Temp. adjustment for release of $NH_4$ sediment rate | 1.080 |
| $\theta_P$ | – | Temp. adjustment for release of $PO_4$ sediment rate | 1.080 |
| $\theta_{bod}$ | – | Temp. adjustment for BOD deoxygenation rate | 1.050 |
| $\theta_{sod}$ | – | Temp. adjustment for oxygen sediment demand rate | 1.080 |
| $\theta_a$ | – | Temp. adjustment for re-aeration rate | 1.028 |
| $f_{ON}$ | – | Fraction of dead phyt. recycled to ON pool | 0.5 |
| $f_{OP}$ | – | Fraction of dead phyt. recycled to OP pool | 0.5 |
| $f_{DON}$ | – | Fraction of dissolved organic nitrogen | 1.0 |
| $f_{DOP}$ | – | Fraction of dissolved organic phosphorus | 1.0 |
| $f_{DBOD}$ | – | Fraction of dissolved CBOD | 1.0 |
| $\alpha_{nc}$ | mgN/mgC | Oxygen to carbon ratio | 0.1 |
| $\alpha_{pc}$ | mgP/mgC | Oxygen to carbon ratio | 0.02 |
| $\alpha_{oc}$ | mgO/mgC | Oxygen to carbon ratio | 2.67 |
| $\alpha_{on}$ | mgO/mgN | Oxygen to nitrogen ratio | 4.57 |
| *cchl* | mgC/mgChl | Phytoplankton carbon to chlorophyll ratio | 50.0 |
| $K_2$ | $m^2/mg$ | Light attenuation coefficient for chlorophyll | 0.002 |
| $k_a$ | 1/d | Re-aeration rate | 0.38 |
| $A$ | $km^2$ | Transversal area of the lake | 36.0 |
| $K_d$ | $m^2/d$ | Vertical eddy diffusivity rate | 0.543 |

## Appendix C

**Table C.1**
Levene's test results for phytoplankton concentration of Paso de las Piedras Reservoirs

| Month | Group | L-critical value | Levene's statistic | p-value |
|---|---|---|---|---|
| Jan. | Cyan. | 3.403 | 1.630 | 0.217 |
| | Green | | 2.309 | 0.121 |
| | Diat. | | 0.129 | 0.879 |
| Feb. | Cyan. | 3.467 | 1.190 | 0.324 |
| | Green | | 2.679 | 0.092 |
| | Diat. | | 2.389 | 0.116 |
| Mar. | Cyan. | 3.403 | 6.801 | 0.005 |
| | Green | | 1.599 | 0.223 |
| | Diat. | | 0.101 | 0.904 |
| Apr. | Cyan. | 3.467 | 0.100 | 0.905 |
| | Green | | 1.371 | 0.276 |
| | Diat. | | 0.089 | 0.915 |
| May | Cyan. | 3.403 | 0.846 | 0.442 |
| | Green | | 4.802 | 0.018 |
| | Diat. | | 3.185 | 0.059 |
| June | Cyan. | 3.467 | 0.428 | 0.657 |
| | Green | | 4.621 | 0.022 |
| | Diat. | | 0.219 | 0.805 |
| July | Cyan. | 3.403 | 0.097 | 0.908 |
| | Green | | 2.993 | 0.069 |
| | Diat. | | 1.369 | 0.273 |
| Aug. | Cyan. | 3.403 | 0.089 | 0.915 |
| | Green | | 2.714 | 0.087 |
| | Diat. | | 0.763 | 0.477 |
| Sept. | Cyan. | 3.403 | 0.494 | 0.616 |
| | Green | | 5.433 | 0.011 |
| | Diat. | | 1.508 | 0.241 |
| Oct. | Cyan. | 3.467 | 3.021 | 0.070 |
| | Green | | 0.425 | 0.660 |
| | Diat. | | 0.175 | 0.841 |
| Nov. | Cyan. | 3.403 | 0.526 | 0.597 |
| | Green | | 0.285 | 0.754 |
| | Diat. | | 0.617 | 0.548 |
| Dec. | Cyan. | 3.403 | 0.030 | 0.971 |
| | Green | | 0.091 | 0.913 |
| | Diat. | | 0.211 | 0.811 |

**Table C.2**
Computational details for parameter estimation problem.

| | TG | FG |
|---|---|---|
| Differential equations | 21 | 29 |
| Initial objective function | 450.89 | 1390.03 |
| Final objective function | 123.84 | −355.13 |
| Iterations | 28 | 106 |
| CPU time (seconds) | 27.56 | 275.84 |
| $X^2$ [a] | 603.56 | 1014.51 |
| Weighted residual | 556.19 | 980.37 |

[a] Good fit: weighted residual less than chi-squared value.

## Appendix D

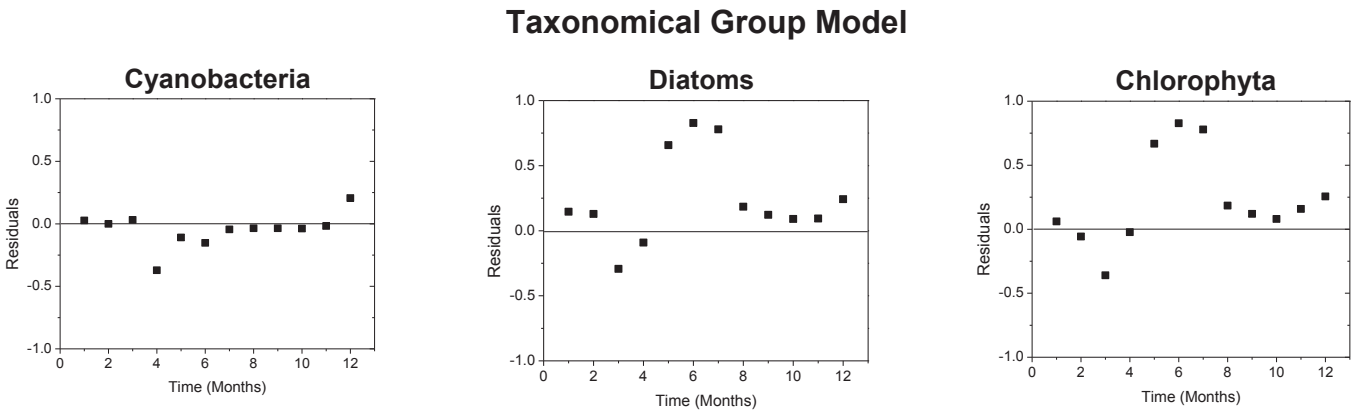


**Fig. D.1.** Residual plot showing the monthly mean of the residuals for phytoplankton variables of the taxonomic group model against time for the calibration period.

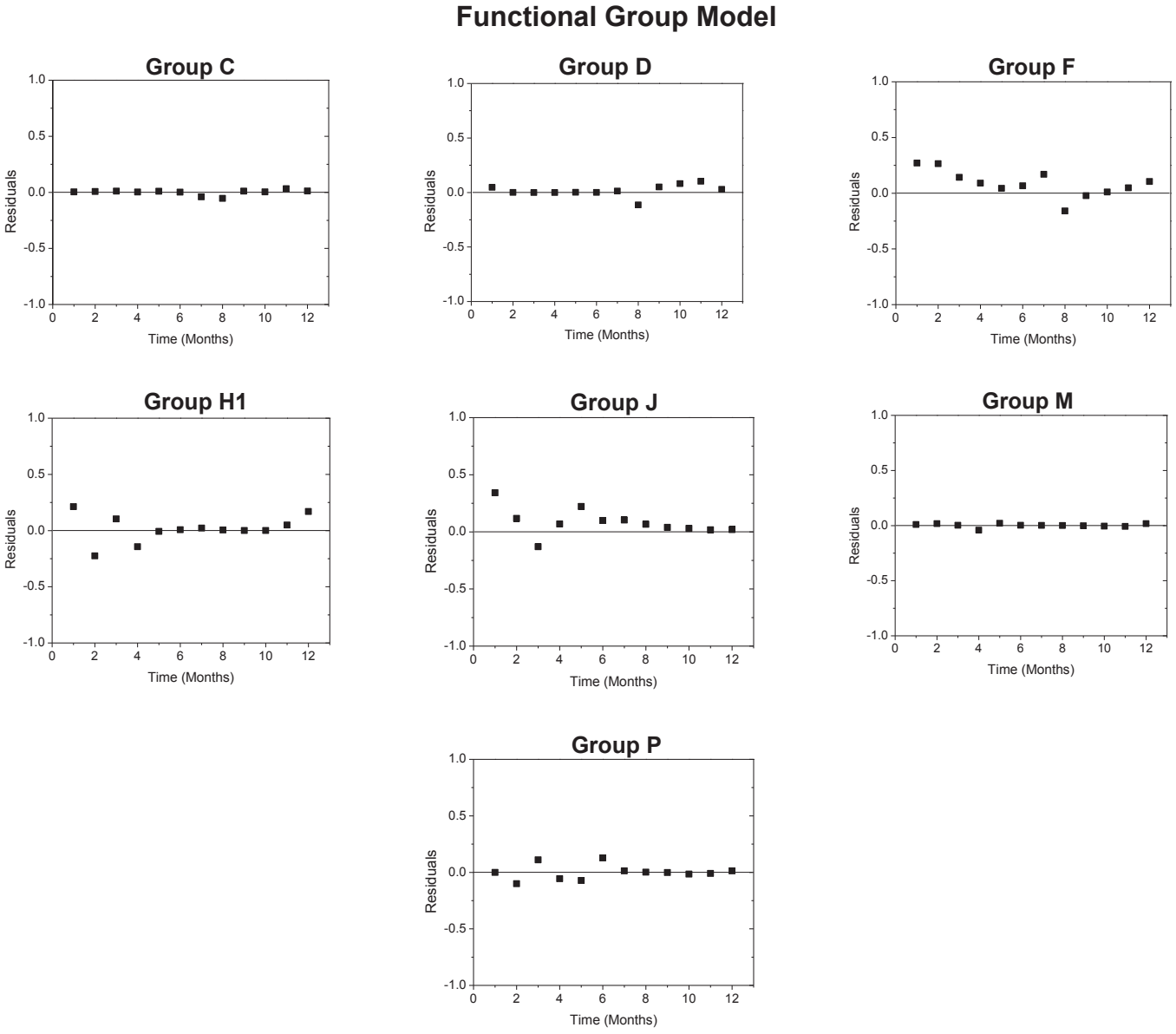


**Fig. D.2.** Residual plot showing the monthly mean of the residuals for phytoplankton variables of the functional group model against time for the calibration period.

## Appendix E

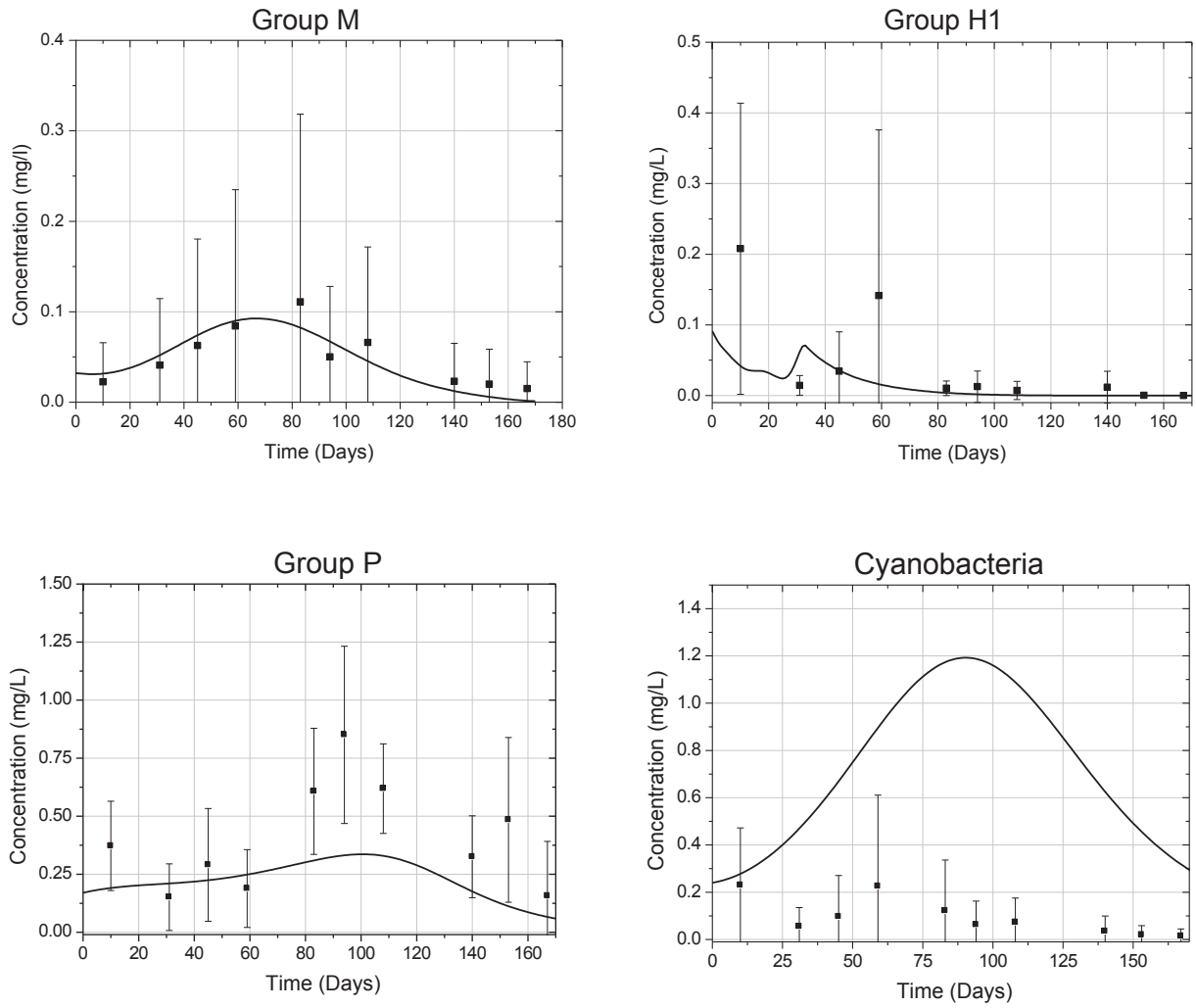


**Fig. E.1.** Validation: observed data (mean and standard deviation) and time series for the four sampling station for group M (a), group H1 (b) and group P (c) of the functional group approach and for cyanobacteria concentration (d) for the taxonomic approach.

## References


APHA, 1992. Standard Methods for the Examination of Water and Wastewater, eighteenth ed. American Public Health Association, Washington, DC.

APHA, AWWA, WPCF, 1989. Standard Methods for the Examination of Water and Wastewater, seventh ed. American Public Health Association Publ, USA.

Alves-de-Souza, C., Menezes, M., Huszar, V., 2006. Phytoplankton composition and functional groups in a tropical humic coastal lagoon, Brazil. Acta Bot. Brasliensis 20, 701–708.

Alves-de-Souza, C., González, M.T., Iriarte, J.L., 2008. Functional groups in marine phytoplankton assemblages dominated by diatoms in fjords of southern Chile. J. Plankton Res. 30, 1233–1243.

Arhonditsis, G.B., Brett, M.T., 2005a. Eutrophication model for Lake Washington (USA): part. I. Model description and sensitivity analysis. Ecol. Model. 187, 140–178.

Arhonditsis, G.B., Stow, C.A., Steinberg, L.J., Kenney, M.A., Lathrop, R.C., McBride, S.J., Reckhow, K.H., 2006. Exploring ecological patterns with structural equation modeling and Bayesian analysis. Ecol. Model. 192, 385–409.

Asaeda, T., Van Bon, T., 1997. Modeling the effects of macrophytes on algal blooming in eutrophic shallow lakes. Ecol. Model. 104, 262–267.

Becker, V., Caputo, L., Ordóñez, J., Marcé, R., Armengol, J., Crossetti, L.O., Huszar, L.M., 2010. Driving factors of the phytoplankton functional groups in a deep Mediterranean reservoir. Water Res. 44, 3345–3354.

Bennett, N., Croke, B., Guariso, G., Guillaume, J., Hamilton, S., Jakeman, A., Marsili-Libelli, S., Newham, L., Norton, J., Perrin, C., Pierce, S., Robson, B., Seppelt, R., Voinov, A., Fath, B., Andreassian, V., 2013. Characterising performance of environmental models. Environ. Model. Softw. 40, 1–20.

Bonnet, M.P., Poulin, M., 2002. Numerical modeling of the planktonic succession in a nutrient-rich reservoir: environmental and physiological factors leading to *Microcystis aeruginosa* dominance. Ecol. Model. 156, 92–112.

Bormans, M., Ford, P.W., Fabbro, L., 2005. Spatial and temporal variability in cyanobacterial populations controlled by physical processes. J. Plankton Res. 27, 61–70.

Bowen, J.D., Hieronymus, J.W., 2003. A CE-QUAL-W2 model of neuse estuary for total maximum daily load development. J. Water Resour. Plan. Manag. 129, 283–294.

Bruce, L.C., Hamilton, D., Imberger, J., Gal, G., Gophen, M., Zohary, Z., Hambright, K.D., 2006. A numerical simulation of the role of zooplankton in C, N and P cycling in Lake Kinneret, Israel. Ecol. Model. 193, 412–436.

Carmichael, W.W., 1992. Cyanobacterial secondary metabolites-cyanotoxins. J. Appl. Bacteriol. 72, 445–459.

Carmichael, W.W., 1997. The cyanotoxins. Adv. Botanical Res. 27, 211–256.

Cerco, C.F., Cole, T.M., 1994. CE-QUAL-ICM: a Three-dimensional Eutrophication Model, Version 1.0. User's Guide, US Army Corps of EngineersWaterways Experiments Station, Vicksburgh, MS.

Chen, C., Ji, R., Schwab, D.J., Beletsky, D., Fahnenstiel, G.L., Jiang, M., Johengen, T.H., Vanderploeg, H., Eadie, B., Budd, J.W., Bundy, M.H., Gardner, W., Cotner, J., Lavrentyev, P.J., 2002. A model study of the coupled biological and physical dynamics in Lake Michigan. Ecol. Model. 152, 145–168.

Chu, Z., Jin, X., Iwami, N., Inamori, Y., 2007. The effect of temperature on growth characteristics and competitions of *Microcystis aeruginosa* and *Oscillatoria mougeotii* in a shallow, eutrophic lake simulator system. Hydrobiologia 581,

217–223.
Defler, R.V., Belk, R.C., 2004. Algae Detection and Removal Strategies for Drinking Water Treatment Plants. AWWA Research Foundation.
Del Barrio Fernández, P., García Gómez, A., García Alba, J., Álvarez Díaz, C., Revilla Cortezón, J.A., 2012. A model for describing the eutrophication in a heavily regulated coastal lagoon. Application to the Albufera of Valencia (Spain). J. Environ. Manag. 112, 340–352.
Dzialowski, A.R., Smith, V.H., Huggins, D.G., de Noyelles, F., Lima, N.-C., Bakera, D.S., Beurya, J.H., 2009. Development of predictive models for geosmin-related taste and odor in Kansas, USA, drinking water reservoirs. Water Res. 43, 2829–2840.
Estrada, V., Parodi, E.R., Diaz, M.S., 2009a. Determination of biogeochemical parameters in eutrophication models with simultaneous dynamic optimization approaches. Comput. Chem. Eng. 33, 1760–1769.
Estrada, V., Parodi, E.R., Diaz, M.S., 2009b. Addressing the control problem of algae growth in water reservoirs with advanced dynamic optimization approaches. Comput. Chem. Eng. 33, 1598–1613.
Estrada, V., Diaz, M.S., 2010. Global sensitivity analysis in the development of first principle based eutrophication models. Environ. Model. Softw. 25, 1539–1551.
Estrada, V., Di Maggio, J., Diaz, M.S., 2011. Water sustainability: a systems engineering approach to restoration of eutrophic lakes. Comput. Chem. Eng. 35, 1598–1613.
Fasham, M.J.R., 1993. Modelling the marine biota. In: Heimann, M. (Ed.), The Global Carbon Cycle. Springer-Verlag, Berlin, pp. 457–504.
Fernández, C., Parodi, E.R., Cáceres, E.J., 2009. aLimnological characteristics and trophic state of Paso delas Piedras Reservoir: an inland reservoir in Argentina. Lakes Reservoirs Res. Manag. 14, 85–101.
Fernández, C., Parodi, E.R., Cáceres, E.J., 2014. Phytoplankton development in a highly eutrophic lake from the pampa plain of Argentina. A functional approach. Int. J. Environ. Res. 8, 1–14.
Friedrichs, M.A.M., Dusenberry, J.A., Anderson, L.A., Armstrong, R.A., Chai, F., Christian, J.R., Doney, S.C., Dunne, J., Fujii, M., Hood, R., McGillicuddy, D.J., Moore, J.K., Schartau, M., Spitz, Y.H., Wiggert, J.D., 2007. Assessment of skill and portability in regional marine biogeochemical models: role of multiple planktonic groups. J. Geophys. Res. 112, 1–22.
Fonseca, B.M., Bicudo, C.E.M., 2008. Phytoplankton seasonal variation in a shallow stratified eutrophic reservoir (Garcas Pond, Brazil). Hydrobiologia 600, 267–282.
Grime, J.P., 1979. Plant Strategies and Vegetation Processes. John Wiley & Sons, New York, p. 222.
Hangos, K., Cameron, I., 2001. Process Modelling and Model Analysis. Academic Press.
Hillebrand, H., Dürselen, C.D., Kirschtel, D., Pollingher, U., Zohary, T., 1999. Biovolume calculation for pelagic and benthic microalgae. J. Phycol. 35, 403–424.
Hindák, F., 1988. Studies on the chlorococcal algae (Chlorophyceae) IV. Biol. Pr. 34, 1–263.
Hindák, F., 1990. Studies on the chlorococcal algae (Chlorophyceae) V. Biol. Pr. 36, 1–225.
Ho, L., Sawade, E., Newcombe, G., 2012. Biological treatment options for cyanobacteria metabolite removal-A review. Water Res. 46, 1536–1548.
Hongping, H.P., Jianyi, M., 2002. Study on the algal dynamic model for West Lake. Ecol. Model. 148, 67–77.
Hongping, P., Yong, W., 2003. Eutrophication research of West Lake, Hangzhou, China: modelingunder uncertainty. Water Res. 37, 416–428.
Huszar, V.L.M., Caraco, N., 1998. The relationship between phytoplankton composition and physical-chemical variables: a comparison of taxonomic and morphological-functional descriptors in six temperate lakes. Freshw. Biol. 40, 679–696.
Imai, H., Chang, K.H., Kusaba, M., Nakano, S., 2009. Temperature-dependentdominance of *Microcystis* (Cyanophyceae) species: *M. aeruginosa* and *M. wesenbergii*. J. Plankton Res. 31, 171–178.
Intartaglia, C., Sala, S.E., 1989. Variación estacional del fitoplancton en un lago no estratificado: Embalse Paso de las Piedras, Argentina. Rev. Bras. Biol. 49, 873–882.
Ito, S., Yoshie, N., Okunishi, T., Ono, T., Okazaki, Y., Kuwata, A., Hashioka, T., Rose, K.A., Megrey, B.A., Kishi, M.J., Nakamachi, M., Shimizu, Y., Kakehi, S., Saito, H., Takahashi, K., Tadokoro, K., Kusaka, A., Kasai, H., 2010. Application of an automatic approach to calibrate the NEMURO nutrient-phytoplankton-zooplankton food web model in the Oyashio region. Prog. Oceanogr. 87, 186–200.
Joh, G., Choi, Y.S., Shin, J.-K., Lee, J., 2011. Problematic algae in the sedimentation and filtration process of water treatment plants. J. Water Supply 60, 219–230.
Jørgensen, S.E., Jørgensen, L.A., Kamp-Nielsen, L., Mejer, H.F., 1981. Parameter estimation in eutrophication modelling. Ecol. Model. 13, 111–129.
Kim, J.T., Boo, S.M., 2001. Occurrence of *Dyctiosphaerium pulchellum* (Chlorophyceae) bloom in a small pond. Korean J. Limnol. 34, 292–297.
Komárek, J., Agnostidis, K., 1989. Modern approach to the classification system of Cyanophytes.4- Nostocales. Arch. Hydrobiol. Suppl. 82 (1). Algological Studies 56, 247–345.
Komárek, J., Agnostidis, K., 1999. In: Ettl, H., Gärtner, G., Heynig, H., Mollenhauer, D. (Eds.), Sübwasserflora von Mitteleuropa Band 19/1. Cyanoprokaryota. 1. Teil: Chroococcales (Berlin).
Komárek, J., Anagnostidis, K., 2005. Cyanoprokaryota. 2. Oscillatoriales. In: Suesswasserflora Von Mittleeuropa 19/2. Fischer Verlag, Stuttgart, p. 759.
Komárek, J., Fott, B., 1983. Das Phytoplankton des Süsswasser Systematik und Biologie. In: Von Huber - Pestalozzi, E. (Ed.), Chlorophyceae (Grünalgen) Ordnung: Chlorococcales. Schweizerbart'sche Verlagsbuchhandlung (Nägele u Obermiller), Sttugart. Germany, p. 1044.
Krammer, K., Lange-Bertalot, H., 1986. Bacillariophyceae 1 Teil: Naviculaceae. In: Ettl, H., Gärtner, J., Heynig, H., Mollenhauer, D. (Eds.), Die Süßwasserflora von Mitteleuropa. Gustav Fisher Verlag, Stuttgart, p. 876.
Krammer, K., Lange-Bertalot, H., 1988. Bacillariophyceae 2 Teil Bacillariaceae, Epithemiaceae, Surirellaceae. In: Ettl, H., Gärtner, J., Heynig, H., Mollenhauer, D. (Eds.), Die Süßwasserflora von Mitteleuropa. Gustav Fisher Verlag, Stuttgart, p. 596.
Krammer, K., Lange-Bertalot, H., 1991a. Bacillariophyceae 3 Teil: Centrales, Fragilariaceae, Eunotiaceae. In: Ettl, H., Gärtner, J., Heynig, H., Mollenhauer, D. (Eds.), Die Süßwasserflora von Mitteleuropa. Gustav Fisher Verlag, Stuttgart, p. 575.
Krammer, K., Lange-Bertalot, H., 1991b. Bacillariophyceae 4 Teil: Achnanthaceae, Kritische Ergäzungen zu Navicula (Lineolatae) und Gomphonema. In: Ettl, H., Gärtner, J., Heynig, H., Mollenhauer, D. (Eds.), Die Süßwasserflora von Mitteleuropa. Gustav Fisher Verlag, Stuttgart, p. 876.
Kruk, C., Huszar, V.L.M., Peeters, T.H.M., Bonilla, S., Costa, L., Lúrling, M., Reynolds, C.S., Scheffer, M., 2010. A morphological classification capturing functional variation in phytoplankton. Freshw. Biol. 55, 614–627.
Kruk, C., Peeters, E.T.H.M., Van Nes, E.H., Huszar, V.L.M., Costa, L.S., Scheffer, M., 2011. Phytoplankton community composition can be predicted best in terms of morphological groups. Limnol. Oceanogr. 56, 110–118.
Makler-Pick, V., Gorfine, G.G., Hipsey, M.R., Carmel, Y., 2011. Sensitivity analysis of complex ecological models – a new approach. Environ. Model. Softw. 26, 124–134.
Mechling, J.A., Kilham, S.S., 1982. Temperature effects on silicon limited growth of the Lake Michigan diatom *Stephanodiscus minutus* (Bacillariopphyceae). J. Phycol. 18, 199–205.
Mieleitner, J., Reichert, P., 2008. Modelling functional groups of phytoplankton in three lakes of different trophic state. Ecol. Model. 211, 279–291.
Mooij, W.M., Janse, J.H., De Senerpont Domis, L.N., Hülsmann, S., Ibelings, B.W., 2007. Predicting the effect of climate change on temperate shallow lakes with the ecosystem model PCLake. Hydrobiologia 584, 443–454.
Montealegre, R.J., Varreth, J., Steenbergen, K., Moed, J., Machiels, M.J., 1995. A dynamic simulation model for the blooming of *Oscillatoria agardhii* in a monomictic lake. Ecol. Model. 78, 17–24.
Moriasi, D.N., Arnold, J.G., Van Liew, M.W., Bingner, R.L., Harmel, R.D., Veith, T.L., 2007. Model evaluation guidelines for systematic quantification of accuracy in watershed simulation. Am. Soc. Agric. Biol. Eng. 50, 885–900.
Nalewajko, C., Murphy, T.P., 2001. Effects of temperature, and availability ofnitrogen and phosphorus on the abundance of *Dolichospermum* and *Microcystis* in LakeBiwa, Japan: an experimental approach. Limnology 2, 45–48.
Omlin, M., Brun, R., Reitchert, P., 2001a. Biogeochemical model of Lake Zürich: model equations and results. Ecol. Model. 141, 77–103.
Omlin, M., Reitchert, P., Forster, R., 2001b. Biogeochemical model of Lake Zürich: sensitivity, identifiability and uncertainty analysis. Ecol. Model. 141, 105–123.
Osidele, O.O., Beck, M.B., 2004. Food web modeling for investigating ecosystem behavior in large reservoirs of the south-eastern United States: lessons from lake Lanier, Georgia. Ecol. Model. 173, 129–158.
Padisák, J., Reynolds, C.S., 1998. Selection of phytoplankton associations in Lake Balaton, Hungary, in response to eutrophication and restoration measures, with special reference to the cyanoprokaryotes. Hydrobiologia 384, 41–53.
Padisák, J., Cressetti, L.O., Naselli-Flores, L., 2009. Use and misuse in the application of the phytoplankton functional classification: a critical review with updates. Hydrobiologia 621, 1–19.
Palmer, C.M., 1980. Algae and Water Pollution. Castle House Publishers Ltd, England, p. 123.
Parinet, J., Rodriguez, M.J., Sérodes, J., 2010. Influence of water quality on the presence of off-flavour compounds (geosmin and 2-methylisoborneol). Water Res. 44, 5847–5856.
Parodi, E.R., Estrada, V., Trobbiani, N., Argañaraz Bonini, G., 2004. Análisis del estado trófico del Embalse Paso de las Piedras. Ecología en tiempos de Cambio, p. 178.
Petzold, L.R., 1982. A Description of DASSL: a Differential/Algebraic System Solver. Technical report SAND82–8637. Sandia National Laboratory.
Power, M., 1993. The predictive validation of ecological and environmental models. Ecol. Model. 68, 33–50.
Priyantha, N.D.G., Asaeda, T., Saitoh, S., Gotoh, K., 1997. Modelling effects of curtain method on algal blooming in reservoirs. Ecol. Model. 98, 89–104.
PSEnterprise Ltd, 2014. gPROMS Advanced User Guide-release 2.3. Process Systems Enterprise Ltd, London.
Rajar, R., Cetina, M., 1997. Hydrodynamic and water quality modelling: an experience. Ecol. Model. 101, 195–207.
Reynolds, C.S., 1984. The Ecology of Freshwater Phytoplankton. Cambridge University Press, Cambridge, UK.
Reynolds, C.S., 1997. Vegetation Processes in the Pelagic. A Model for Ecosystem-Theory. ECI, Oldendorf.
Reynolds, C.S., Huszar, V., Kruk, C., Naselli-Flores, L., Melo, S., 2002. Towards a functional classification of the freshwater phytoplankton. J. Plankton Res. 24, 417–428.
Reynolds, C.S., 2006. The Ecology of Phytoplankton. Cambridge University Press, Cambridge, p. 535.
Rigosi, A., Marcé, R., Escot, C., Rueda, F.J., 2011. A calibration strategy for dynamic succession models including several phytoplankton groups. Environ. Model. Softw. 26, 697–710.
Rigosi, A., Carey, C.C., Ibelings, B., Brookes, J.D., 2014. The interaction between

climate warming and eutrophication to promote cyanobacteria is dependent ontrophic state and varies among taxa. Limnol. Oceanogr. 59, 99–114.
Riley, M.J., Stefan, H.G., 1988. MINLAKE: a dynamic lake water quality simulation model. Ecol. Model. 43, 155–182.
Robarts, R.D., Zohary, T., 1992. The influence of temperature and light on the upperlimit of *Microcystis aeruginosa* production in a hypertrophic reservoir. J. Ofplankt. Res. 14, 235–247.
Romero, J.R., Antenucci, J.P., Imberger, J., 2004. One- and three-dimensional biogeochemical simulations of two differing reservoirs. Ecol. Model. 174, 142–160.
Rode, M., Suhr, U., Wriedt, G., 2007. Multi-objetive calibration of a river water quality model-Information content of calibration data. Ecol. Model. 204, 129–142.
Rott, E., 1981. Some results from phytoplankton counting intercalibrations. Swiss J. Hydrol. 43, 34–62.
Roy, S., Chattopadhyay, J., 2007. Towards a resolution of "the paradox of the plankton": a brief overview of the proposed mechanisms. Ecol. Complex. 4, 26–33.
Sagehashi, M., Sakoda, A., Suzuki, M., 2000. A predictive model of long-term stability after biomanipulation of shallow lakes. Water Res. 34, 4014–4028.
Salmaso, N.J., Padisák, J., 2007. Morpho-functional groups and phytoplankton development in two deep lakes (Lake Garda, Italy and Lake Stechlin, Germany). Hydrobiologia 578, 97–112.
Scheffer, M., Rinaldi, S., Huisman, J., Weissing, F.J., 2003. Why plankton communities have no equilibrium: solutions to the paradox. Hydrobiologia 491, 9–18.
Schindler, D.W., Hecky, R.E., Findlay, D.L., Stainton, M.P., Parker, B.R., Paterson, M.J., Beaty, K.G., Lyng, M., Kasian, S.E.M., 2008. Eutrophication of lakes cannot be controlled by reducing nitrogen input: results of a 37-year whole-ecosystem experiment. PNAS 105, 11254–11258.
Segura, A.M., Kruk, C., Calliari, D., Fort, H., 2013. Use of a morphology-based functional approach to model phytoplankton community succession in a shallow subtropical lake. Freshw. Biol. 58, 504–512.
Seinfeld, J.H., Lapidus, L., 1974. Mathematical Methods in Chemical Engineering. In: Process Modeling,estimation and Identification, vol. 3. Prentice-Hall, INC, Englewood Cliffs, New Jersey.
Smayda, T.J., 1978. From phytoplankters to biomass. In: Sournia, A. (Ed.), Phytoplankton Manual. Oxford UNESCO, Paris, pp. 273–280.
Smayda, T.J., Reynolds, C.S., 2001. Community assembly in marine phytoplankton: application of recent models to harmful dinoflagellate blooms. J. Plankton Res. 23, 447–461.
Smayda, T.J., Reynolds, C.S., 2003. Strategies of marine dinoflagellate survival and some rules of assembly. J. Sea Res. 49, 95–106.
Sun, J., Liu, D., 2003. Geometric models for calculating cell biovolume and surface area for phytoplankton. J. Plankton Res. 25, 1331–1346.
Tucker, C.S., Llyod, S.W., 1984. Phytoplankton communities in channel catfish ponds. Hydrobiologia 112, 137–141.
Utermöhl, H., 1958. Zur Vervollkommmung der quantitative Phytoplankton-Methodik. Mitt.int. Verein. theor. angew. Limnology 5, 567–596.
Vollenweider, R.A., 1975. Input-output models with special reference to the phosphorus loading concept in limnology. Schweiz. z. Hydrol. 37, 53–84.
Wetzel, R.G., 2001. Limnology: Lake and River Ecosystems, 3ra. ed. Academic Press, New York, USA.
Willmott, C.J., 1981. On the validation of models. Phys. Geogr. 2, 184–194. http://dx.doi.org/10.1080/02723646.1981.10642213.
Wyatt, T., 2013. Margalef's Mandala and Phytoplankton Bloom Strategies. Deep-Sea Res. II. http://dx.doi.org/10.1016/j.dsr2.2012.12.006.
Zhang, J., Jørgensen, S.E., Mahler, H., 2004. Examination of structurally dynamic eutrophication model. Ecol. Model. 173, 313–333.
Zheng, L., Chen, C., Zhang, F.Y., 2004. Development of water quality model in the Satilla River Estuary, Georgia. Ecol. Model. 178, 457–482.
Zhao, J., Ramin, M., Cheng, V., Arhonditsis, G.B., 2008b. Competition patterns among phytoplankton groups: How useful are the complex mathematical models. Acta Oecol. 33.